Title
DISSECTING PAIN AND ITCH CIRCUITS IN THE CENTRAL NERVOUS SYSTEM

Permalink
https://escholarship.org/uc/item/7g59946x

Author
Wercberger, Racheli

Publication Date
2019

Peer reviewed|Thesis/dissertation

Dissecting Pain and Itch Circuits in the Central Nervous System

by
Racheli Wercberger

DISSERTATION
Submitted in partial satisfaction of the requirements for degree of
DOCTOR OF PHILOSOPHY

in

Neuroscience

in the

GRADUATE DIVISION
of the
UNIVERSITY OF CALIFORNIA, SAN FRANCISCO

Approved:

Zachary Knight
                                                                                    Chair

Allan Basbaum

Peter Ohara
Peter Ohara

David Julius

Committee Members

Dedication and Acknowledgements

I'd like to thank Dr. Allan Basbaum for providing incredible support throughout my time as a graduate student in his lab. I couldn't have completed this difficult work of getting a PhD without his constant mentorship and kind encouragement. I'd also like to acknowledge the members of my thesis (and qualifying exam) committee, Zack Knight, David Julius, and Peter Ohara, for providing guidance on my project year after year. Big thanks to the members of the Basbaum lab, past and present, who have been excellent coworkers and also contributed to the evolution of this work through countless lab meetings. In particular, I want to thank Joao Braz for being my lab mentor and collaborator on this project, as well as Jarret Weinrich for completely revolutionizing the way I think about and analyze data, including in this project. I am so grateful, too, for Karuna Meda, who has been such a good friend and source of support throughout my time in the lab, even after she graduated and left the lab. I certainly wouldn't be here without the endless support that I get from my chosen family, including Jenna Whippen, Kit Solowy, Yael Schonzeit, and Abby Krumbein, as well as my parents, siblings, and nibblings. And finally, I want to dedicate this work to my dear friend, Cris Alvaro, whose beauty and magic were unparalleled and whose presence inside and outside the lab shaped my world in more ways than I can ever express.

Dissecting pain and itch circuits in the central nervous system

Racheli Wercberger

Abstract

Almost one in five American adults suffers from chronic pain, and millions suffer from chronic itch, yet our understanding of the circuits that underlie pain and itch remain elusive. Specifically, it is unclear whether pain and itch are transmitted along distinct, so-called labeled line neuronal pathways ("specificity") or if algogenic (pain- provoking) and pruritogenic (itch-provoking) inputs converge on a single circuit ("convergence"). There is unquestionably complex molecular and functional heterogeneity at the level of the primary sensory neurons—as well as second order, spinal cord dorsal horn interneurons— with discrete populations of neurons transmitting modality-specific pain or itch signals. That organization suggests that specificity predominates. However, whether there is specificity or convergence at the level of the dorsal horn projection neurons, which carry the message to the brain, where the pain or itch percept is eventually established, is unclear. To date the great majority of studies have relied almost exclusively on expression of the neurokinin 1 receptor (NK1R), which responds to the neuropeptide, substance P, to define the neurochemistry of projection neurons. However, as the NK1R is expressed by the majority of projection neurons, it is not a suitable molecular marker to determine whether there are functionally specific subpopulations.

Our objective was to more comprehensively profile the molecular complexity of projection neurons and to determine if subpopulations are more relevant to the transmission of pain or itch messages. To this end, in the mouse we isolated populations of projection neurons that target the parabrachial nucleus of the brainstem, a major relay in the transmission of pain and itch messages to the brain.   From these projection neurons, we generated two RNA sequencing datasets of differentially expressed genes that are enriched in projection neurons compared to all neurons in the dorsal horn of the spinal cord and in the trigeminal nucleus caudalis, which processes information from the face. Among many genes enriched in the projection neurons, we focused our analysis on several that have already been implicated in pain and/or itch processing, including *Cck*, *Nptx2*, *Nmb*, and *Crh*. Importantly, these genes have not previously been associated with projection neurons. By multiple labeling *in situ* hybridization studies of the expression of these enriched genes, combined with retrograde labeling of projection neurons and pain- and itch-stimulus induced *Fos* expression, we have demonstrated that there are molecularly distinct subpopulations of projection neurons, based on their expression of the enriched genes, their spatial location, and their responsiveness to pain and itch-provoking stimulation. Corroborating electrophysiological and morphological data in the literature showing the heterogeneity of dorsal horn projection neurons, we conclude that projection neurons are diverse, and as such the NK1R is not the ideal marker to interrogate subpopulation function. The database of enriched genes identified and characterized in this study should permit more precise dissection of pain and itch circuits in the central nervous system going forward.

Table of Contents

List of Figures

List of Tables

Chapter 1

Introduction to the Neurobiology of Pain and Itch

Pain and itch are independent somatosensory sensations, yet they are also linked, with overlapping as well as distinct characteristics. In an acute setting, they are both defined as "unpleasant sensory and emotional experience[s] associated with actual or potential tissue damage" (in the case of pain) (Anon, n.d.) or "disruption to the skin" (in the case of itch) (Davidson and Giesler, 2010). Both experiences include an impulse or motivation to respond to the provoking stimulus, although the stimuli and behavioral responses for pain and itch are distinct: pain-provoking stimuli (algogens) typically produce a withdrawal response (avoidance of the stimulus) while itch-provoking stimuli (pruritogens) produce an impulse to scratch. Despite the fact that algogens and pruritogens are different chemically, and that pain and itch are perceptually and behaviorally discrete, their molecular and neural underpinnings are nevertheless often difficult to distinguish from one another. For example, most neurons that transmit pain and itch messages are polymodal, that is, they have receptors for and are activated by both algogens and pruritogens (Basbaum et al., 2009). Technological advances have enabled researchers to dissect the circuits underlying the transmission of pain and itch-provoking messages with increasing precision, but there is still much unknown regarding how sensory discrimination is achieved. In other words, how does the brain generate independent pain and itch percepts from circuits that have convergent, polymodal properties? In this chapter, we provide a brief overview of the current state of pain and itch circuit research, from the periphery to the brain. Chapter 2 focuses

specifically on the projection neurons, namely the neurons that receive the algogenic and pruritogenic inputs and transmit these inputs to the brain.

General Pain and Itch Circuitry

Pain (mechanical, thermal, and chemical) and itch sensations are evoked by algogenic and pruritic stimuli, respectively, which engage specific receptors at the peripheral terminals of the primary sensory neuron, or primary afferent fiber. These terminals innervate skin, muscle, and viscera. The sensory neuron is unusual morphologically as its cell body is located just outside of the spinal cord, in the dorsal root ganglion, and it has both the latter peripheral axon branch as well as a central branch that terminates in the dorsal horn of the spinal cord. Sensory neurons that innervate the face are comparable, with cell bodies in the trigeminal ganglion and a central branch that innervates the nucleus caudalis of the medulla, which is the homologue of the dorsal horn. In the spinal cord dorsal horn and trigeminal nucleus caudalis (TNC), the central branch of the primary afferent fibers engage interneurons and projection neurons, which carry "pain" and "itch" messages to the brain.

Importantly, there is extensive modulation of the incoming messages to the spinal cord by local excitatory and inhibitory interneurons, as well as by descending systems that can either facilitate or inhibit the signals before they leave the cord. The projection neurons reach supraspinal targets, predominately via axons that course in the anterior lateral funiculus white matter. Broadly, the sensory discriminatory aspects of pain and itch (e.g. quality, intensity, and location) are transmitted via the ascending

trigeminothalamic (TTT) and spinothalamic tract (STT) to the ventral basal thalamus, and from there, to primary somatosensory cortex (Melzack and Casey, 1968; Almeida et al., 2004; Dostrovsky and Craig, 2010; Lima, 2010). The affective and motivational components of pain and itch (e.g. the degree of unpleasantness) are chiefly transmitted through circuits that engage the medial and intralaminar thalamic nuclei, and limbic regions, including the amygdala, insular cortex, and the anterior cingulate cortex (ACC) (Vogt and Sikes, 2000; Almeida et al., 2004; Lima, 2010). Not surprisingly, the pain and itch percepts generated are not merely a function of the magnitude of the particular algogenic or pruritogenic stimuli. Rather, cognitive processes including attention, stress, and expectation can affect the magnitude of the experience, which illustrates the incredible complexity involved in the translation of stimulus to perception (Wiech et al., 2008; Villemure and Bushnell, 2009).

Theories of Transmission

A major objective in sensory neuroscience is to determine how the brain discriminates among different sensory modalities. For example, although algogenic and pruritic messages must be transferred to the brain to be perceived as pain or itch, respectively, the extent to which the transmitted information is segregated remains unclear. Two opposing neural mechanisms as to how this occurs predominate. Specificity theory proposes that discrete neural circuits, or labeled-lines, carry information of a specific input modality (e.g., noxious mechanical, thermal, or pruritic), from the peripheral afferents to the spinal cord and by modality specific projection neurons to the brain. Pattern theory, in contrast, posits that the brain integrates convergent input from various

sensory modalities and generates a distinct perceptual output based on the pattern of firing of projection neurons (**Fig. 1.1**).

In support of the former, labeled-line theory is the fact that many primary afferents respond selectively to noxious mechanical, thermal, or itch-provoking stimuli (Cavanaugh et al., 2009; Liu et al., 2009; Han et al., 2013; Knowlton et al., 2013). For example, primary afferents expressing the MrgprD receptor, a member of the Mas-related G-protein coupled receptor family, contribute to behavioral responses to noxious mechanical, but not thermal, stimuli, while those that express TRPV1, a member of the transient receptor potential (TRP) family of receptors, are indispensable for painful heat-evoked behaviors (Cavanaugh et al., 2009). Similarly, afferents that express TRPM8, another member of the TRP family, are essential for cool and noxious cold-evoked behaviors (Knowlton et al., 2013), and those that express MrgprA3 apparently only signal itch (Han et al., 2013).

There are also many molecularly defined subsets of spinal interneurons that selectively transmit pain or itch messages. For example, excitatory interneurons that express gastrin-releasing peptide (GRP) or its receptor (GRPR) and inhibitory interneurons that express the transcription factor Bhlhb5 appear to trigger itch, but not pain behavior (Sun and Chen, 2007; Sun et al., 2009; Ross et al., 2010), while a circuit involving inhibitory dynorphin-expressing interneurons and somatostatin-expressing excitatory interneurons has recently been implicated in the behavioral response to noxious mechanical stimuli

(Duan et al., 2014). However, the fact that the Bhlhb5- and dynorphin-expressing neurons belong to largely overlapping populations complicates these results.

Clearly the interneurons do not send messages to the brain. Rather, they engage the projection neurons and importantly the specificity in the peripheral afferents and spinal cord interneurons is much less apparent among the projection neurons. While there are nociceptive-specific projection neurons (which may be polymodal with respect to pain processing, but not responsive to pruritogens)(Christensen and Perl, 1970; Davidson et al., 2012) as well as small numbers of pruriceptive-specific projection neurons (Andrew and Craig, 2001; Akiyama et al., 2010), either of which might convey modality specificity to the brain, most data suggest that signals of different pain and itch modalities converge on most projection neurons. In fact, electrophysiological studies of antidromically activated projection neurons shows that the majority of projection neurons are polymodal with respect to pain and itch. (Simone et al., 2004; Davidson et al., 2012; Moser and Giesler, 2014; Jansen and Giesler, 2015). Furthermore, chemical ablation of a majority of projection neurons, which express the neurokinin 1 receptor (NK1R), results in the reduction of *both* pain and itch behaviors (Mantyh et al., 1997; Carstens et al., 2010). This finding suggests either that inputs converge on the projection neurons, or that there are subsets of NK1R expressing cells that carry modality-specific information. Unfortunately, the paucity of known molecular markers that selectively label dorsal horn projection neurons makes it difficult to distinguish between these two possibilities. Clearly, before we can conclude that pain and itch inputs converge or remain segregated at the level of the projection neurons, it is crucial

to determine whether there are molecularly and functionally distinct subpopulations of projection neurons. The subsequent chapters focus on this problem in more depth.

Although many of the above findings support a labeled-line system, there is evident cross-talk, if not convergence, between pain and itch circuits, as shown by the polymodal electrophysiology of individual neurons at all levels of the neuraxis, including projection neurons. Of particular interest are the well-documented phenomena of noxious heat-, cold-, or mechanical-induced (e.g., scratching) suppression of itch (Bromma et al., 1995; Ward et al., 1996; Vierow et al., 2009; McCoy et al., 2013; Kardon et al., 2014). Additionally, some analgesics, notably morphine, reduce pain while increasing itch, particularly when administered at the spinal cord level. This finding is true in both humans and rodents. This cross-modal modulation suggests a more complex neural circuit than could be accounted for by a simple labeled-line model.

A third hypothesis for how pain and itch are transmitted to the brain accounts for this complexity. The population code theory (**Fig. 1.1**) posits that there are labeled-lines, such that, if a given labeled-line is activated in isolation and under normal conditions, it would generate sensation of a discrete modality (Ma, 2012). However, the population code theory also takes into consideration the fact that many sensory neurons are polymodal. As a result, a particular stimulus (e.g. heat) could activate several labeled-lines. Finally, the population code posits that labeled-lines "talk" to one another. As a result the different labeled lines have the capability of modulating the activity of other lines, through direct and interneuronal connections. In other words, under normal

physiological conditions, it is the balance of activation and cross-talk between and among lines that determines which sensory labeled-line is ultimately conveyed.

Summary

In the following chapters, we focus in more detail on the projection neurons of the spinal cord dorsal horn and TNC. Chapter 2 provides an in-depth background of the projection neuron literature, and in subsequent chapter(s) we present the findings from our current experiments. Specifically, by profiling dorsal horn projection neurons our objective is to classify molecular and functional subtypes.
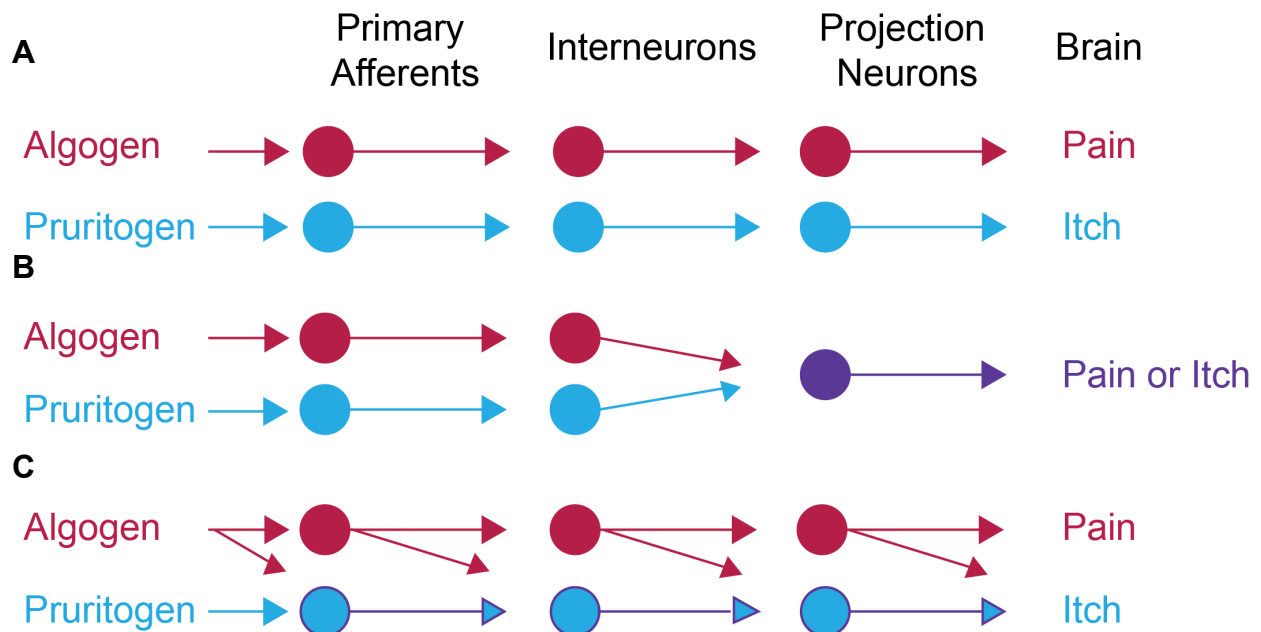
Figure 1.1: Summary of theories of pain and itch transmission
(A) The Labeled-Line theory suggests that there are discrete neural pathways that underlie transmission of a single modality from the periphery to the brain, while **(B)** Pattern theory or Convergence suggests that different modalities, i.e. pain and itch, converge on to a modality nonspecific circuit. In the latter case, the brain generates sensory discrimination by decoding the pattern of activity of the projection neurons, which would differ depending on the stimulus. The schematic shows convergence only at the level of the projection neuron to reflect the evidence that many primary afferents and interneurons are specific for a given modality. **(C)** The Population Code theory suggests that there is cross talk between labeled-lines, so that cells may be polymodal or have convergent inputs, but that they nevertheless transmit specific information to the brain. According to this theory, the brain generates modality discrimination by reading the input across populations of projection neurons.

References

Akiyama T, Carstens MI, Carstens E (2010) Facial injections of pruritogens and
algogens excite partly overlapping populations of primary and second-order
trigeminal neurons in mice. J Neurophysiol 104:2442–2450.

Almeida TF, Roizenblatt S, Tufik S (2004) Afferent pain pathways: A neuroanatomical
review. Brain Res 1000:40–56.

Andrew D, Craig AD (2001) Spinothalamic lamina I neurons selectively sensitive to
histamine: a central neural pathway for itch. Nat Neurosci 4:72–77.

Anon (n.d.) IASP Terminology - IASP. Available at: https://www.iasp-
pain.org/Education/Content.aspx?ItemNumber=1698 [Accessed May 16, 2019].

Basbaum AI, Bautista DM, Scherrer G, Julius D (2009) Cellular and Molecular
Mechanisms of Pain. Cell. 139:267-84.

Bromma B, Scharein E, Darsow U, Ring J (1995) Effects of menthol and cold on
histamine-induced itch and skin reactions in man. Neurosci Lett. 187(3):157-60.

Carstens EE, Carstens MI, Simons CT, Jinks SL (2010) Dorsal horn neurons
expressing NK-1 receptors mediate scratching in rats. Neuroreport 21:303–308.

Cavanaugh DJ, Lee H, Lo L, Shields SD, Zylka MJ, Basbaum AI, Anderson DJ (2009)

> Distinct subsets of unmyelinated primary sensory fibers mediate behavioral

> responses to noxious thermal and mechanical stimuli. Proc Natl Acad Sci U S A.

> 106:9075-80.

Christensen B, Perl ER (1970) Spinal neurons specifically excited by noxious or thermal

> stimuli: marginal zone of the dorsal horn. J Neurophysiol 33:293–307.

Davidson S, Giesler GJ (2010) The multiple pathways for itch and their interactions with

> pain. Trends Neurosci 33:550–558.

Davidson S, Zhang X, Khasabov SG, Moser HR, Honda CN, Simone DA, Giesler GJ,

> Jr. (2012) Pruriceptive spinothalamic tract neurons: physiological properties and

> projection targets in the primate. J Neurophysiol 108:1711–1723.

Dostrovsky JO, Craig AD (2010) The Thalamus and Nociceptive Processing. In: The

> Senses: A Comprehensive Reference. 5:635-54.

Duan B, Cheng L, Bourane S, Britz O, Padilla C, Garcia-Campmany L, Krashes M,

> Knowlton W, Velasquez T, Ren X, Ross SE, Lowell BB, Wang Y, Goulding M, Ma

> Q (2014) Identification of spinal circuits transmitting and gating mechanical pain.

> Cell. 159:1417-32.

Han L, Ma C, Liu Q, Weng HJ, Cui Y, Tang Z, Kim Y, Nie H, Qu L, Patel KN, Li Z, McNeil B, He S, Guan Y, Xiao B, Lamotte RH, Dong X (2013) A subpopulation of nociceptors specifically linked to itch. Nat Neurosci 16:174–182.

Jansen NA, Giesler GJ (2015) Response characteristics of pruriceptive and nociceptive trigeminoparabrachial tract neurons in the rat. J Neurophysiol 113:58–70.

Kardon AP et al. (2014) Dynorphin Acts as a Neuromodulator to Inhibit Itch in the Dorsal Horn of the Spinal Cord. Neuron. 82:573-586.

Knowlton WM, Palkar R, Lippoldt EK, McCoy DD, Baluch F, Chen J, McKemy DD (2013) A Sensory-Labeled Line for Cold: TRPM8-Expressing Sensory Neurons Define the Cellular Basis for Cold, Cold Pain, and Cooling-Mediated Analgesia. J Neurosci. 33:2837-48.

Lima D (2010) Ascending Pathways: Anatomy and Physiology. In: The Senses: A Comprehensive Reference. 5:477-526.

Liu Q, Tang Z, Surdenikova L, Kim S, Patel KN, Kim A, Ru F, Guan Y, Weng HJ, Geng Y, Undem BJ, Kollarik M, Chen ZF, Anderson DJ, Dong X (2009) Sensory Neuron-Specific GPCR Mrgprs Are Itch Receptors Mediating Chloroquine-Induced Pruritus. Cell. 139:1353-65.

Ma Q (2012) Population coding of somatic sensations. Neurosci Bull 28:91–99

Mantyh PW, Rogers SD, Honore P, Allen BJ, Ghilardi JR, Li J, Daughters RS, Lappi DA, Wiley RG, Simone DA (1997) Inhibition of hyperalgesia by ablation of lamina I spinal neurons expressing the substance P receptor. Science 278:275–279

McCoy ES, Taylor-Blake B, Street SE, Pribisko AL, Zheng J, Zylka MJ (2013) Peptidergic CGRPα Primary Sensory Neurons Encode Heat and Itch and Tonically Suppress Sensitivity to Cold. Neuron. 78:138-51.

Melzack R, Casey KL (1968) Sensory, Motivational, and Central Control Determinants of Pain: A New Conceptual Model. In: The Skin Senses: Proceedings of the First International Symposium on the Skin Senses. 423-439.

Moser HR, Giesler GJ (2014) Characterization of pruriceptive trigeminothalamic tract neurons in rats. J Neurophysiol 111:1574–1589.

Ross SE et al. (2010) Loss of Inhibitory Interneurons in the Dorsal Spinal Cord and Elevated Itch in Bhlhb5 Mutant Mice. Neuron. 65:886-98.

Simone DA, Zhang X, Li J, Zhang J-M, Honda CN, LaMotte RH, Giesler GJ (2004) Comparison of responses of primate spinothalamic tract neurons to pruritic and algogenic stimuli. J Neurophysiol 91:213–222.

Sun YG, Chen ZF (2007) A gastrin-releasing peptide receptor mediates the itch sensation in the spinal cord. Nature. 448:700-703.

Sun YG, Zhao ZQ, Meng XL, Yin J, Liu XY, Chen ZF (2009) Cellular basis of itch sensation. Science. 325:1531-4.

Vierow V, Fukuoka M, Ikoma A, Dörfler A, Handwerker HO, Forster C (2009) Cerebral Representation of the Relief of Itch by Scratching. J Neurophysiol. 102:3216-24.

Villemure C, Bushnell MC (2009) Mood Influences Supraspinal Pain Processing Separately from Attention. J Neurosci. 29:705-15.

Vogt BA, Sikes RW (2000) The medial pain system, cingulate cortex, and parallel processing of nociceptive information. In: Progress in Brain Research. 122:223-35.

Ward L, Wright E, McMahon SB (1996) A comparison of the effects of noxious and innocuous counterstimuli on experimentally induced itch and pain. Pain. 64:129-38.

Wiech K, Ploner M, Tracey I (2008) Neurocognitive aspects of pain perception. Trends

Cogn Sci. 12:306-13.

Chapter 2

Spinal and Medullary Dorsal Horn Projection Neurons

Recent studies have described a plethora of neurochemically-distinct primary afferent and spinal cord interneuron populations, several of which are tuned to discrete pain and itch stimulus modalities (Todd, 2010; Braz et al., 2014; LaMotte et al., 2014; Peirs and Seal, 2016; Koch et al., 2018). However, whether and to what extent this specificity extends to the dorsal horn projection neurons is unclear. Are distinct modalities conveyed by labeled-lines, by convergence and coding of the signals, or a combination of both?

A labeled-line hypothesis necessitates the existence of functionally distinct subpopulations of projections neurons. In support of this hypothesis, based on morphology, electrophysiology, projection targets, and neurochemistry, there is considerable evidence of projection neuron heterogeneity. As yet, however, there is no comprehensive atlas of the molecular profiles of discrete projection neuron populations. As a result, and despite evidence to the contrary, projection neurons are often regarded as a relatively homogeneous group. In this chapter, we integrate conclusions from classical as well as contemporary studies and provide a thorough view of the diversity of the projection neurons that carry nociceptive and pruriceptive information to the brain, emphasizing the extent to which there is evidence for modality-specific subpopulations, and highlighting gaps in our knowledge.

Projection neurons: what do we know?

Projection neurons that transmit pain- and itch-relevant information to the brain originate throughout the spinal cord and in its homologue in the medulla, the trigeminal nucleus caudalis (TNC). These two regions carry information from the body and face, respectively. At both sites, there is a dense population of projection neurons in lamina I; others are scattered throughout laminae III-VIII, X and in the lateral spinal nucleus (LSN) (Todd, 2010; Braz et al., 2014). Together, these neurons give rise to several ascending pathways that terminate widely, in the nucleus of the solitary tract (NTS), the medial brainstem reticular formation, the caudal ventrolateral medulla (CVLM), the lateral parabrachial nucleus (LPb), the midbrain periaqueductal gray (PAG) and the thalamus and hypothalamus (Almeida et al., 2004; Todd, 2010). Importantly, many projection neurons have propriospinal collaterals that terminate intersegmentally in the spinal cord (Szucs et al., 2010; Gutierrez-Mecinas et al., 2018). Most projections are to contralateral loci, however, bilateral, and to a lesser extent, ipsilateral projections have been described (Spike et al., 2003). In the current and next chapters, we focus on projection neurons in the dorsal half of the spinal cord and TNC.

Lamina-specific evidence of projection neuron heterogeneity

Before reviewing the literature an important caveat must be emphasized. It is almost impossible to establish a consensus as to the functional heterogeneity of spinal and medullary projection neurons. Some studies were performed in decerebrate or spinalized preparations, and many under anesthesia, which can impact normal physiological function. Some studies characterized the properties of antidromically-

activated projection neurons; others did not. Many studies report on data obtained from very few cells, and unquestionably, there are species differences. Finally, few studies examined the properties of projection neurons in chronic injury settings where, for example, injury-induced neurochemical changes in sensory neurons, including non-nociceptive A-beta afferents, can significantly alter the properties of dorsal horn neurons (Woolf et al., 1998).

LAMINA I

The classification of morphological subtypes of projection neurons in lamina I highlighted three major categories, defined by somatodendritic architecture: fusiform, pyramidal, and multipolar (Lima and Coimbra, 1986; Zhang et al., 1996; Zhang and Craig, 1997). Many studies probed whether these morphological subtypes correlate with specific physiological properties (Han et al., 1998), ascending projection (Lima and Coimbra, 1988, 1989; Lima et al., 1991), or receptor expression (Yu et al., 1999; Almarestani et al., 2007). Unfortunately, the correlations are inconsistent (Todd et al., 2002, 2005; Spike et al., 2003). Lamina I projection neurons target the thalamus, LPb, CVLM and the PAG, and in the mouse, ~90% can be retrogradely labeled from the LPb, demonstrating a high degree of collateralization (Spike et al., 2003; Al-Khater and Todd, 2009). Dendrites of the majority of these projection neurons arborize in lamina I, where they receive direct input from nociresponsive C- and Aδ-fibers (Christensen and Perl, 1970; Willis et al., 1974; Bester et al., 2000; Todd et al., 2002; Torsney and MacDermott, 2006; Saeed and Ribeiro-da-Silva, 2012). Importantly, although some lamina I neurons respond to heat, pinch and noxious cold (HPC) (Han et al., 1998),

others, namely the nociceptive-specific (NS) neurons, are more selective, responding only to noxious pinch and/or heat and have different intrinsic properties (Craig et al., 2001). Lamina I also contains wide dynamic range (WDR) neurons that respond in a graded manner to innocuous as well as noxious mechanical, thermal, and pruritic stimulation (Craig and Kniffki, 1985; Hylden et al., 1986; Bester et al., 2000; Davidson et al., 2012; Moser and Giesler, 2014; Jansen and Giesler, 2015), and some lamina I spinothalamic tract (STT) neurons in monkey (Dostrovsky and Craig, 1996) and cat (Craig et al., 2001) respond selectively to innocuous cooling. Recently, in the mouse, lamina I spinoparabrachial neuron subpopulations, with varying degrees of modality selectivity, were characterized, with one population responding exclusively to noxious cold (Hachisuka et al., 2016).

Perhaps the strongest claim for specificity comes from Craig and colleagues, who described in the cat, lamina I STT populations that respond exclusively to discrete stimuli, e.g., histamine (Andrew and Craig, 2001a), innocuous cooling (Craig et al., 2001) or warming (Andrew and Craig, 2001b). However, these conclusions were based on relatively few cells, and subsequent studies in monkey (Simone et al., 2004; Davidson et al., 2012) and rat (Moser and Giesler, 2014) could not confirm these findings. Nevertheless, despite evidence for predominantly polymodal projection neurons, some subpopulations may transmit differential, functionally relevant information. For example, in the monkey, among lamina I nociceptive neurons are pruriceptive populations that differentially respond to histamine and cowage (Davidson et al., 2012). And interestingly, in the rat, trigeminothalamic (VTT) neurons that respond

to both pruritogens and algogens are differentially influenced by morphine, compared to VTT neurons that respond exclusively to algogenic stimuli (Moser and Giesler, 2013). Our own laboratory reported that morphine only suppresses noxious stimulus-evoked Fos expression in a subpopulation of rat spinoparabrachial neurons (Jasmin et al., 1994). Many of these opioid effects are likely indirect, via superficial dorsal horn interneuron circuitry, which provides yet another mechanism for functionally segregating the properties of subpopulations of lamina I projection neurons.

LAMINAE III-V

Early, pain-relevant electrophysiological studies in the cat (Wall, 1967) and primate (Willis Jr., 1985) focused on wide dynamic range (WDR) neurons in deep dorsal horn (lamina V). Other studies described spinocervical tract cells in laminae III-IV, which likely constitute a parallel "pain" transmission network (Iggo et al., 1985). In fact, not until Christensen and Perl (1970) described nociceptive specific neurons in lamina I did attention turn dramatically away from the deep dorsal horn.

Laminae III-V projection neurons are generally multipolar, with long, dorsally-directed dendrites that can extend to lamina I. As a result, they receive input from primary afferents that terminate throughout the superficial dorsal horn, including a significant low threshold Aβ myelinated input (Price et al., 1978; De Koninck et al., 1992; Torsney and MacDermott, 2006). Some of these projection neurons express the neurokinin 1 receptor (NK1R) (Brown et al., 1995) and receive a convergent nociceptive input from substance P (SP)-containing afferents (Naim et al., 1997), and likely also from local

interneurons (Gutierrez-Mecinas et al., 2017). Importantly, many spinal and medullary projection neurons in laminae III-V respond robustly to pruritogens (Davidson et al., 2012; Moser and Giesler, 2014; Jansen and Giesler, 2015). Some WDR neurons in laminae III-V are somatotopically organized (Willis Jr., 1985; Price et al., 2003), which would provide a substrate for stimulus localization and intensity coding. Interestingly, in a translational study comparing rats and humans, the graded firing response of lamina V neurons to increasing stimulus intensity correlated with human intensity reports (Sikandar et al., 2013).

LATERNAL SPINAL NUCLEUS (LSN)

Located in the white matter of the rodent dorsal horn, lateral to lamina I, the LSN extends along the rostrocaudal length of the spinal cord, and is replaced at the most rostral cervical levels by the neurochemically-distinct lateral cervical nucleus (Giesler and Elde, 1985). Many LSN neurons express the NK1R (Ding et al., 1995), but in contrast to those in laminae I and III-IV, they do not receive a direct primary afferent input. Rather, they receive a polysynaptic, neurochemically rich peptidergic input, including interneuronal and propriospinal-derived SP (Jiang et al., 1999; Gutierrez-Mecinas et al., 2018). The LSN neurons project to brainstem, hypothalamus, and thalamus (Todd, 2010), and collateralize within the spinal dorsal horn, and they convey nociceptive information mainly from deep somatic and visceral structures (Sikandar et al., 2017).

Conclusion

There is a remarkable diversity of projection neuron populations in the spinal cord and TNC. However, the organizational principles that define this diversity, or as Piers and Seal (2016) write, "the logic of the projection neuron populations" remains a mystery. We conclude here that the evidence for convergence of multiple modalities onto the projection neurons is overwhelming. Most projection neurons that respond to pruritogens also respond to algogens, most projection neurons that respond to noxious heat also respond to noxious mechanical stimulation, and many neurons that respond to pain-provoking inputs also respond to innocuous stimulation. We do not find compelling the claims that modality-specific percepts arise from spinal cord or medullary projection neurons that strictly respond to and convey information of a single modality, particularly since the latter constitute no more than 5% of the population (Andrew and Craig, 2001b, 2001a; Akiyama et al., 2010). Thus, the question remains: how does the brain interpret convergent information so as to generate percepts that are clearly different? One suggestion, mentioned in the previous chapter, is that the brain interprets a "population code" generated by activity across polymodal projection neurons (Ma, 2012). In this formulation, although there is limited specificity as to the modality to which an individual projection neuron responds, there is specificity in the modality information that a population of neurons can convey. This broader interpretation of labeled-lines has been demonstrated with the TRPV1-positive sensory neurons that co-express MRGPRA3 (Han et al., 2013). When selectively activated, this TRPV1 subpopulation of afferents conveys itch rather than noxious heat, despite their polymodal responsiveness to heat, capsaicin and pruritogens. Ultimately, a comprehensive atlas of dorsal spinal cord and

TNC projection neurons must be delineated if we are to understand how different pain and itch modalities are processed, and how the information that the projection neurons transmit results in distinct percepts.

Summary

In the following chapter, we present the findings from our current experiments, in which we profiled dorsal horn projection neurons in order to classify molecular and functional subtypes. We used an adapted protocol of translating ribosome affinity purification (TRAP) to tag ribosomes of spinal and medullary dorsal horn neurons that project to the lateral parabrachial nucleus (LPb). With this method we were able to purify ribosomes and their associated mRNA from projection neurons of the dorsal spinal cord and TNC and then characterize their molecular profiles by RNA-sequencing. We generated two datasets of genes enriched either in all spinoparabrachial neurons or in the NK1R-expressing subset of spinoparabrachial neurons. We also confirmed and characterized the expression of several new marker genes, as well as the responsiveness to puritogens and algogens of the projection neurons that express these markers. The databases we generated will enable development of subtype-specific tools for their functional manipulation, including cell ablation, and allow more precise dissection of ascending pain and itch-provoking circuits.

References

Akiyama T, Carstens MI, Carstens E (2010) Facial injections of pruritogens and
algogens excite partly overlapping populations of primary and second-order
trigeminal neurons in mice. J Neurophysiol 104:2442–2450.

Al-Khater KM, Todd AJ (2009) Collateral projections of neurons in laminae I, III, and IV
of rat spinal cord to thalamus, periaqueductal gray matter, and lateral parabrachial
area. J Comp Neurol 515:629–646.

Almarestani L, Waters SM, Krause JE, Bennett GJ, Ribeiro-da-Silva A (2007)
Morphological characterization of spinal cord dorsal horn lamina I neurons
projecting to the parabrachial nucleus in the rat. J Comp Neurol 504:287–297.

Almeida TF, Roizenblatt S, Tufik S (2004) Afferent pain pathways: A neuroanatomical
review. Brain Res 1000:40–56.

Andrew D, Craig AD (2001a) Spinothalamic lamina I neurons selectively sensitive to
histamine: a central neural pathway for itch. Nat Neurosci 4:72–77.

Andrew D, Craig AD (2001b) Spinothalamic lamina I neurones selectively responsive to
cutaneous warming in cats. J Physiol 537:489–495.

Bester H, Chapman V, Besson J-M, Bernard J-F (2000) Physiological Properties of the Lamina I Spinoparabrachial Neurons in the Rat. J Neurophysiol 83:2239–2259.

Braz J, Solorzano C, Wang X, Basbaum A (2014) Transmitting Pain and Itch Messages: A Contemporary View of the Spinal Cord Circuits that Generate Gate Control. Neuron. 82:522-36.

Brown JL, Liu H, Maggio JE, Vigna SR, Mantyh PW, Basbaum AI (1995) Morphological characterization of substance P receptor-immunoreactive neurons in the rat spinal cord and trigeminal nucleus caudalis. J Comp Neurol 356:327–344.

Christensen B, Perl ER (1970) Spinal neurons specifically excited by noxious or thermal stimuli: marginal zone of the dorsal horn. J Neurophysiol 33:293–307.

Craig AD, Kniffki KD (1985) Spinothalamic lumbosacral lamina I cells responsive to skin and muscle stimulation in the cat. J Physiol 365:197–221.

Craig AD, Krout K, Andrew D (2001) Quantitative response characteristics of thermoreceptive and nociceptive lamina I spinothalamic neurons in the cat. J Neurophysiol 86:1459–1480.

Davidson S, Zhang X, Khasabov SG, Moser HR, Honda CN, Simone DA, Giesler GJ, Jr. (2012) Pruriceptive spinothalamic tract neurons: physiological properties and projection targets in the primate. J Neurophysiol 108:1711–1723.

De Koninck Y, Ribeiro-da-Silva A, Henry JL, Cuello AC (1992) Spinal neurons exhibiting a specific nociceptive response receive abundant substance P-containing synaptic contacts. Proc Natl Acad Sci U S A 89:5073–5077.

Ding Y-Q, Takada M, Shigemoto R, Mizuno N (1995) Spinoparabrachial tract neurons showing substance P receptor-like immunoreactivity in the lumbar spinal cord of the rat. Brain Res 674:336–340.

Dostrovsky JO, Craig AD (1996) Cooling-specific spinothalamic neurons in the monkey. J Neurophysiol 76:3656–3665.

Giesler G, Elde R (1985) Immunocytochemical studies of the peptidergic content of fibers and terminals within the lateral spinal and lateral cervical nuclei. J Neurosci 5:1833–1841.

Gutierrez-Mecinas M, Bell AM, Marin A, Taylor R, Boyle KA, Furuta T, Watanabe M, Polgár E, Todd AJ (2017) Preprotachykinin A is expressed by a distinct population of excitatory neurons in the mouse superficial spinal dorsal horn including cells that respond to noxious and pruritic stimuli. Pain 158:440–456.

Gutierrez-Mecinas M, Polgár E, Bell AM, Herau M, Todd AJ (2018) Substance P-expressing excitatory interneurons in the mouse superficial dorsal horn provide a propriospinal input to the lateral spinal nucleus. Brain Struct Funct 223:2377–2392

Hachisuka J, Baumbauer KM, Omori Y, Snyder LM, Koerber HR, Ross SE (2016) Semi-intact ex vivo approach to investigate spinal somatosensory circuits. Elife 5:1–19.

Han L, Ma C, Liu Q, Weng HJ, Cui Y, Tang Z, Kim Y, Nie H, Qu L, Patel KN, Li Z, McNeil B, He S, Guan Y, Xiao B, Lamotte RH, Dong X (2013) A subpopulation of nociceptors specifically linked to itch. Nat Neurosci 16:174–182.

Han Z-S, Zhang E-T, Craig AD (1998) Nociceptive and thermoreceptive lamina I neurons are anatomically distinct. Nat Neurosci 1:218–225.

Hylden JLK, Hayashi DRH, Dubner R, Bennett GJ (1986) Physiology and morphology of the lamina I spinomesencephalic projection. J Comp Neurol 247:505–515.

Iggo A, Steedman WM, Fleetwood-Walker S (1985) Spinal processing: anatomy and physiology of spinal nociceptive mechanisms. Philos Trans R Soc London 308:235–252.

Jansen NA, Giesler GJ (2015) Response characteristics of pruriceptive and nociceptive trigeminoparabrachial tract neurons in the rat. J Neurophysiol 113:58–70.

Jasmin L, Wang H, Tarczy-Hornoch K, Levine JD, Basbaum AI (1994) Differential

    effects of morphine on noxious stimulus-evoked fos-like immunoreactivity in

    subpopulations of spinoparabrachial neurons. J Neurosci 14:7252–7260.

Jiang MC, Liu L, Gebhart GF (1999) Cellular properties of lateral spinal nucleus neurons

    in the rat L6-S1 spinal cord. J Neurophysiol 81:3078–3086.

Koch SC, Acton D, Goulding M (2018) Spinal circuits for touch, pain, and itch. Annu Rev

    Physiol 80:189–217.

LaMotte RH, Dong X, Ringkamp M (2014) Sensory neurons and circuits mediating itch.

    Nat Rev Neurosci 15:19–31.

Lima D, Coimbra A (1986) A Golgi study of the neuronal population of the marginal

    zone (lamina I) of the rat spinal cord. J Comp Neurol 244:53–71.

Lima D, Coimbra A (1988) The spinothalamic system of the rat: Structural types of

    retrogradely labelled neurons in the marginal zone (lamina I). Neuroscience

    27:215–230.

Lima D, Coimbra A (1989) Morphological types of spinomesencephalic neurons in the marginal zone (Lamina I) of the rat spinal cord, as shown after retrograde labelling with cholera toxin subunit B. J Comp Neurol 279:327–339.

Lima D, Mendes-Ribeiro JA, Coimbra A (1991) The spino-latero-reticular system of the rat: Projections from the superficial dorsal horn and structural characterization of marginal neurons involved. Neuroscience 45:137–152.

Ma Q (2012) Population coding of somatic sensations. Neurosci Bull 28:91–99.

Moser HR, Giesler GJ (2013) Itch and analgesia resulting from intrathecal application of morphine: contrasting effects on different populations of trigeminothalamic tract neurons. J Neurosci 33:6093–6101.

Moser HR, Giesler GJ (2014) Characterization of pruriceptive trigeminothalamic tract neurons in rats. J Neurophysiol 111:1574–1589.

Naim M, Spike RC, Watt C, Shehab SA, Todd AJ (1997) Cells in laminae III and IV of the rat spinal cord that possess the neurokinin-1 receptor and have dorsally directed dendrites receive a major synaptic input from tachykinin-containing primary afferents. J Neurosci 17:5536–5548.

Peirs C, Seal RP (2016) Neural circuits for pain: Recent advances and current views. Science 354:578–584.

Price DD, Greenspan JD, Dubner R (2003) Neurons involved in the exteroceptive function of pain. Pain 106:215–219.

Price DD, Hayes RL, Ruda M, Dubner R (1978) Spatial and temporal transformations of input to spinothalamic tract neurons and their relation to somatic sensations. J Neurophysiol 41:933–947.

Saeed AW, Ribeiro-da-Silva A (2012) Non-peptidergic primary afferents are presynaptic to neurokinin-1 receptor immunoreactive lamina I projection neurons in rat spinal cord. Mol Pain 8 Available at: http://journals.sagepub.com/doi/10.1186/1744-8069-8-64.

Sikandar S, Ronga I, Iannetti GD, Dickenson AH (2013) Neural coding of nociceptive stimuli - From rat spinal neurones to human perception. Pain 154:1263–1273.

Sikandar S, West SJ, McMahon SB, Bennett DL, Dickenson AH (2017) Sensory processing of deep tissue nociception in the rat spinal cord and thalamic ventrobasal complex. Physiol Rep. 5(14).

Simone DA, Zhang X, Li J, Zhang J-M, Honda CN, LaMotte RH, Giesler GJ (2004)
Comparison of responses of primate spinothalamic tract neurons to pruritic and
algogenic stimuli. J Neurophysiol 91:213–222.

Spike RC, Puskár Z, Andrew D, Todd AJ (2003) A quantitative and morphological study
of projection neurons in lamina I of the rat lumbar spinal cord. Eur J Neurosci
18:2433–2448.

Szucs P, Luz LL, Lima D, Safronov B V. (2010) Local axon collaterals of lamina I
projection neurons in the spinal cord of young rat. J Comp Neurol 518:2645–2665
Available at: http://doi.wiley.com/10.1002/cne.22391.

Todd AJ (2010) Neuronal circuitry for pain processing in the dorsal horn. Nat Rev
Neurosci 11:823–836.

Todd AJ, Puskar Z, Spike RC, Hughes C, Watt C, Forrest L (2002) Projection neurons
in lamina I of rat spinal cord with the neurokinin 1 receptor are selectively
innervated by substance p-containing afferents and respond to noxious stimulation.
J Neurosci 22:4103–4113.

Todd AJ, Spike RC, Young S, Puskár Z (2005) Fos induction in lamina I projection
neurons in response to noxious thermal stimuli. Neuroscience 131:209–217.

Torsney C, MacDermott AB (2006) Disinhibition Opens the Gate to Pathological Pain

    Signaling in Superficial Neurokinin 1 Receptor-Expressing Neurons in Rat Spinal

    Cord. J Neurosci 26:1833–1843.

Wall PD (1967) The laminar organization of dorsal horn and effects of descending

    impulses. J Physiol 188:403–423.

Willis Jr. WD (1985) Pain pathways in the primate. Prog Clin Biol Res 176:117–133.

Willis WD, Trevino DL, Coulter JD, Maunz RA (1974) Responses of primate

    spinothalamic tract neurons to natural stimulation of hindlimb. J Neurophysiol

    37:358–372.

Woolf CJ, Mannion RJ, Neumann S (1998) Null Mutations Lacking Substance:

    Elucidating Pain Mechanisms by Genetic Pharmacology. Neuron 20:1063–1066.

Yu XH, Zhang ET, Craig AD, Shigemoto R, Ribeiro-da-Silva A, De Koninck Y (1999)

    NK-1 receptor immunoreactivity in distinct morphological types of lamina I neurons

    of the primate spinal cord. J Neurosci 19:3545–3555.

Zhang E-T, Craig AD (1997) Morphology and distribution of spinothalamic lamina I

    neurons in the monkey. J Neurosci 17:3274–3284.

Zhang E-T, Han Z-S, Craig AD (1996) Morphological classes of spinothalamic lamina I neurons in the cat. J Comp Neurol 367:537–549.

Chapter 3

Molecular Profiling of Dorsal Horn Projection Neurons

INTRODUCTION

An important objective of sensory neuroscience is to acquire the molecular language that defines cell-type specificity, so as to map neural circuits with precision. Toward this end, recent studies have extensively characterized the molecular heterogeneity that underlies pain and itch circuits, predominantly at the level of the peripheral primary afferents as well as the spinal interneurons, both of which are comprised of many molecularly defined functional subpopulations. There is also abundant electrophysiological and morphological evidence for heterogeneity of the dorsal horn projection neurons, which carry pain and/or itch messages to the brain. To illustrate their diversity, electrophysiological studies have found that many projection neurons in lamina I are nociceptive specific (some of which respond to noxious mechanical stimuli, thermal, or both)(Christensen and Perl, 1970; Han et al., 1998; Bester et al., 2000; Craig et al., 2001; Hachisuka et al., 2016) while others respond only to innocuous cooling (Dostrovsky and Craig, 1996; Craig et al., 2001). Anatomical studies identified three distinct morphological classes of lamina I projection neurons(Lima and Coimbra, 1986; Zhang et al., 1996; Zhang and Craig, 1997), and there is some, albeit controversial, evidence for the correlation of morphology with the electrophysiological profile of these cells (Han et al., 1998), as well as their ascending projections (Lima and Coimbra, 1988, 1989; Lima et al., 1991) and receptor expression (Yu et al., 1999;

Almarestani et al., 2007). There are also many projection neurons in both superficial and deeper laminae that are wide dynamic range (WDR) cells, responding to brush, touch, and pinch (Wall, 1967; Craig and Kniffki, 1985; Willis Jr., 1985; Hylden et al., 1986; Bester et al., 2000). A subset of these neurons is pruriceptive, with separate populations responding to the pruritogens histamine and cowage (Simone et al., 2004; Davidson et al., 2007, 2012, 2014; Jansen and Giesler, 2015). However, as virtually all of these neurons also respond to mechanical stimuli and some to noxious heat, the evidence for modality specific populations is limited.

Despite the apparent functional heterogeneity of dorsal horn projection neurons, they are often regarded in the literature as a homogenous group. This is likely due to the fact that there are very few, if any, molecular markers that can distinguish among functional subpopulations. With few exceptions (see below), the neurokinin 1 receptor (NK1R, or *Tacr1*), which is targeted by the neuropeptide substance P (SP), remains the marker consistently used to define projection neurons and even to interrogate their contribution to pain and itch (Mantyh et al., 1997; Carstens et al., 2010). In rat and mouse, ~80 and 90% of lamina I projection neurons, respectively, express the receptor (Ding et al., 1995; Marshall et al., 1996; Todd et al., 2000; Cameron et al., 2015), as does the majority (70%) of spinoparabrachial neurons in the lateral spinal nucleus (LSN) (Ding et al., 1995). Fewer projection neurons in laminae III-V express the NK1R (~33% of STT neurons in the rat (Marshall et al., 1996), and 44% of spinoparabrachial neurons in the mouse (Cameron et al., 2015)). The relatively small number of NK1R-negative projection neurons in lamina I, which have large, multipolar cell bodies, are defined

molecularly only by gephyrin puncta and expression of the glycine α1 (GlyRα1) and GluR4 AMPA receptor subunits (Puskár et al., 2001; Polgár et al., 2008). As yet, however, the functional significance of this differential molecular make-up is not clear.

The fact that the great majority of projection neurons express the NK1R effectively reduces its utility as a molecular marker for a functionally discrete population. In fact, to categorize molecularly the heterogeneity of the projection neurons, we need to determine whether there are molecular subsets of the NK1R-expressing neurons. There has been some progress toward this end. For example, a subset of lamina I neurons that project to the nucleus of the solitary tract (NTS) in the rat (Gamboa-Esteves et al., 2004), and about 10% of NK1R-expressing spinoparabrachial neurons in the mouse (Cameron et al., 2015) double label for the sst2A somatostatin receptor. Whether these represent functionally distinct subtypes is not known. Interestingly, some NK1R-expressing lamina I spinoparabrachial neurons in the cat (Blomqvist and Mackerlova, 1995) and mouse (Cameron et al., 2015) express SP, which could, in an autoreceptor fashion, presynaptically modulate neurotransmission at terminal targets. Most recently, Huang et al. (2019) found SP-expressing NK1R-positive neurons in lamina I that project to the superior lateral parabrachial nucleus (LPb) and medial thalamic nuclei. The authors proposed that these neurons contribute selectively to a thalamocortical circuit that underlies complex behavioral responses to ongoing pain, rather than reflex responses to acute noxious stimuli. Despite the latter advances and as mentioned above, dorsal horn projection neurons are still often conflated into one group, likely due to the poor molecular resolution that we have to define subpopulations.

More recently, RNA-sequencing has systematically and with great sensitivity defined molecularly diverse populations of dorsal horn neurons. For example, using unbiased single cell transcriptomics, Häring et al. (2018) delineated 15 excitatory and 15 inhibitory categories of dorsal horn neurons, and by combining retrograde tracing with in situ hybridization (ISH), confirmed that spinoparabrachial neurons are concentrated in the NK1R-defined (*Tacr1*) Glut 15 excitatory cluster. This cluster included many other molecular markers, e.g., *Lypd1*, a forebrain protein previously implicated in anxiety disorders (Tekinay et al., 2009). However, as *Lypd1* labels ~95% of spinoparabrachial projection neurons (Häring et al., 2018), it likely does not define a functionally distinct subset.

To achieve a more focused analysis of the molecular profiles of NK1R-positive and -negative dorsal horn projection neurons, we have taken a projection neuron-centric approach to RNA-sequencing. Using retro-TRAP (translating ribosome affinity purification), we purified spinoparabrachial neurons and generated RNA-seq datasets of candidate marker genes for projection neurons. Here we identified and characterized marker genes that have not previously been associated with projection neurons. To develop a molecular and correlated functional database of projection neurons, we tested the responsiveness of the newly-defined projection neuron populations to various pain- and itch-provoking stimuli. This database will enable development of subtype-specific tools for cell ablation and manipulation and allow more precise dissection of ascending pain and itch circuits.

RESULTS

Selective purification and profiling of projection neuron RNA from precipitated tagged-ribosomes:

To purify and sequence RNA specifically from projection neurons, we modified an approach (Ekstrand et al., 2014) that tags ribosomes of neurons based on their projection target for later immunoprecipitation (IP) and sequencing (**Fig. 3.1A**). Our analysis took advantage of the fact that ~90% of all lamina I projection neurons target or collateralize in the lateral parabrachial nucleus (LPb) (Spike et al., 2003; Al-Khater and Todd, 2009; Todd, 2010). Here we bilaterally injected a replication deficient, retrograde herpes simplex virus (HSV)-based viral vector encoding a green fluorescent protein (GFP)-tagged large ribosomal subunit protein L10 (HSV-GFPL10) into the LPb of wildtype mice to induce expression of GFP-L10 in projection neurons. In a parallel study, we injected an HSV-based viral vector encoding a cre-recombinase dependent HA-tagged L10 (HSV-flex-HAL10) into the LPb of NK1R-cre mice. In these experiments, expression of HA-L10 is induced selectively in LPb-projecting neurons that express the NK1R, as compared to all (NK1R- and non-NK1R-expressing) projection neurons recovered in the first set of experiments. The data obtained from animals injected with HSV-GFPL10 are hereafter referred to as the "PN" dataset, as that experiment should have captured any projection neuron (PN) that targets the LPb. Data from the RNA from animals injected with HSV-flex-HAL10 are referred to as the "NK" dataset, as only

NK1R-expressing (NK) dorsal horn projection neurons were captured in those experiments.

We recorded GFP- and HA-tagged ribosomes in projection neurons throughout the spinal cord and trigeminal nucleus caudalis (TNC) in wildtype (**Fig. 3.1B**) and in NK1R-cre (**Fig. 3.1C**) mice, respectively. Consistent with the distribution pattern of spinal cord and TNC projection neurons, we observed GFP- and HA-positive cells in Lamina I, III-V, X and in the lateral spinal nucleus (LSN).

To purify ribosomes and associated mRNA from projection neurons, we dissected dorsal spinal cord and TNC tissue and immunoprecipitated ribosomes fused to GFP or HA. For the Input control, we used total mRNA from homogenized dorsal spinal cord and TNC. Consistently, the RNA yields from the IPs performed on tissue from injected animals were at least one order of magnitude greater than IPs performed on tissue from uninjected controls (data not shown), and we detected 18S and 28S rRNA peaks from the former samples only (**Supplemental Fig. 3.1A**), suggesting that the ribosomal tag was necessary to pull down RNA and that the IPs were specific for projection neurons.

As a further confirmation of the specificity of the IP, we performed Taqman qPCR and tested for enrichment of *Gfp* or *Tacr1* mRNA in the IP relative to the Input samples. There was robust enrichment of *Gfp* (64.6-fold average enrichment; p<0.0001; **Fig. 3.1D**, **Supplemental Fig. 3.1B**) and an enrichment of two-fold or higher of *Tacr1* (26.5-fold average enrichment; **Fig. 3.1E**, **Supplemental Fig. 3.1C**) in all libraries.

Depletion of glial markers also confirmed specificity of the projection neuron IPs. The

following glial markers were significantly depleted in the PN IPs: mbp (6.4-fold average

depletion), mal (3.9-fold), and slc1a2 (7.0-fold)(p<0.005; **Fig. 3.1F**, **Supplemental Fig.**

3.1D). Glial marker genes were similarly depleted in NK IPs relative to Input: mbp (4.2-

fold; p<0.05), mal (5.4-fold; p<0.0001), slc1a2 (1.2-fold) (**Fig. 3.1G**, **Supplemental Fig.**

3.1D).

RNA sequencing and differential expression reveals candidates for projection neuron

marker genes:

To identify marker genes that define projection neurons, we performed RNA sequencing

on all IP and Input libraries, and used differential expression analysis to determine

which genes are enriched in the projection neuron IPs relative to the dorsal spinal cord

and TNC Input.

To compare the PN and NK datasets, we plotted the gene fold changes within each

dataset against the other (**Fig. 3.1H**). Data points in quadrants one (Q1) and three (Q3)

represent transcripts that were enriched or depleted in projection neurons in both

datasets, while those in quadrants two (Q2) and four (Q4) represent transcripts that are

differentially enriched or depleted. As ~90% of all lamina I spinoparabrachial neurons

express NK1R (Spike et al., 2003; Al-Khater and Todd, 2009), we expected both

datasets to be largely overlapping and thus the majority of data points should lie in Q1

and Q3. This was indeed what we observed. Importantly, however, the transcripts in Q2

and Q4, and particularly those in Q4, provide a valuable (albeit limited) list of potential markers for the non-NK1R expressing projection neurons, for which there are currently no or only very limited marker genes identified (**Supplemental Table 3.2)**.

Genes that are significantly enriched or depleted in the IPs from the PN (green), NK (blue) or both datasets (red) are plotted (**Fig. 3.1H, Supplemental Figs. 3.2A, B**). *Tacr1* is enriched in both datasets, and as expected it is much more highly enriched in the NK dataset. These results suggest that the PN dataset contains a relatively high proportion of non-NK1R projection neurons, and/or that there is a relatively high amount of NK1R-expressing interneurons in the Input samples, which would reduce the relative enrichment of the projection neurons in the PN dataset. The latter also implies that the *Tacr1* enrichment in the NK dataset is underestimated.

To validate the enrichment of the candidate marker-genes from the RNA-seq datasets, we performed qPCR on cDNA from the IP and Input samples obtained from both the PN and NK experiments (**Supplemental Figs. 3.1E, F**) and confirmed enrichment of the majority of hits in the IP relative to Input samples. For the remainder of this report, we have focused on several genes that were enriched in both PN and NK RNA-seq and qPCR datasets (in yellow, Q1, **Fig. 3.1H, Supplemental Figs. 3.1E, F, Supplemental Figs. 3.2A, B**). The particular candidates have some prior mention in pain and/or itch literature, but have not been emphasized with respect to projection neuron neurochemistry.

RNA sequencing identifies marker genes expressed by projection neurons:

We were particularly intrigued by the enrichment of *Cck* in both PN and NK datasets.

Cck encodes cholecystokinin, a peptide that in preclinical studies has been implicated

as an anti-opioid (Faris et al., 1983; Watkins et al., 1985). In fact, Cck antagonists used

clinically have been reported to potentiate morphine analgesia (McCleane, 2004) as

well as placebo analgesia (Benedetti and Amanzio, 1997). Several studies report *Cck*

expression in excitatory interneurons in the dorsal horn (Häring et al., 2018; Gutierrez-

Mecinas et al., 2019), but there is limited evidence of its expression in projection

neurons (Leah et al., 1988). To investigate the latter question, we labeled

spinoparabrachial neurons throughout the TNC by injecting HSV-GFPL10 bilaterally in

LPb and performed double fluorescent ISH on TNC tissue, for *Gfp* and *Cck*. Figure

3.2A illustrates *Cck*-expressing neurons in laminae II, III and IV, with many fewer in

lamina I (**Fig. 3.2A**). Based on the presence or absence of co-labeling with the *Gfp*

retrograde marker, we conclude that the great majority of these cells are interneurons.

Importantly however, we did record numerous examples of *Cck*-expressing projections

neurons

(**Fig. 3.2A**).

The neuronal pentraxin 2 (*Nptx2*) gene, also called Narp, encodes a secreted protein

that is involved in excitatory synaptogenesis, and has been implicated in anxiety,

Alzheimer's Disease and schizophrenia (Chang et al., 2018). Its connection to pain

processing, however, is limited. *Nptx2* expression is expressed in sensory neurons

and has been implicated in the microglial response to nerve injury (Miskimon et al.,

2014).

Whether *Nptx2* is expressed in the TNC or dorsal horn, and whether it is expressed in projection neurons has not been established. Here we recovered *Gfp*-expressing spinoparabrachial neurons that co-express *Nptx2*, predominantly in laminae I and III/IV, a distribution pattern typical of dorsal horn projection neurons (**Fig. 3.2B**). As for *Cck*, however, the high number of *Nptx2*-expressing neurons suggests that the population includes both projection neurons and interneurons.

Neuromedin B (*Nmb*) is a neuropeptide member of the bombesin-like family of peptides. *Nmb* has been implicated in thermal nociception (Mishra et al., 2012), and in the processing of itch messages (Su and Ko, 2011; Fleming et al., 2012; Wan et al., 2017). The expression of *Nmb* in sensory neurons is robust, and although there are reports of its expression in the spinal cord, the types of neuron in which it is expressed has not been investigated (Fleming et al., 2012). Here, we found that *Nmb* is expressed sparsely in the TNC, predominantly in superficial laminae, and that these neurons are a subset of the *Gfp*-labeled spinoparabrachial neurons (**Fig. 3.2C**).

Corticotropin-releasing hormone (*Crh*), also referred to as corticotropin-releasing factor (*Crf*), is best studied through its contribution to the HPA-axis (Hypothalamus-pituitary-adrenal) and stress. However there is also evidence that *Crh* can regulate pain processing centrally as well as peripherally. For example, in preclinical studies, intracranial administration of *Crh* produced analgesia in several pain assays (Lariviere and Melzack, 2000). *Crh* can also indirectly decrease pain by acting as an anti-inflammatory agent at the site of injury (Hargreaves et al., 1989; Lariviere and Melzack,

2000). Consistent with our finding that *Crh* is enriched in both PN and NK projection neuron datasets, Häring et al. (2018) reported that *Crh* is expressed in an excitatory neuron cluster, namely the Glut15 cluster, which included spinoparabrachial neurons. Figure 3.2D shows that *Crh* is expressed predominantly in the superficial laminae neurons of the TNC, where it overlaps with Gfp-labeled spinoparabrachial neurons (**Fig. 3.2D**).

Projection neurons in both superficial and deep dorsal horn express enriched genes:

Electrophysiological studies of pain-relevant projection neurons, largely performed in cat and monkey, focused on lamina V wide dynamic range (WDR) neurons as well as lamina III and IV neurons at the origin of the spinocervical tract (Wall, 1967; Iggo et al., 1985; Willis Jr., 1985). Not until Christensen and Perl described nociceptive specific projection neurons in lamina I (1970) did attention turn to the superficial dorsal horn (sDH). Today, despite the early electrophysiological studies, as well as several reports of NK1R-expressing projection neurons in deep dorsal horn (dDH) (Brown et al., 1995), there is a strong bias towards studying lamina I projection neurons, often to the exclusion of those located ventrally. To redress this bias, here we characterized projection neurons in both superficial and deep dorsal horn and TNC that express the different enriched genes (**Fig. 3.3**). Interestingly, in both dorsal horn and TNC, *Cck* is expressed by a higher percentage of deep projection neurons relative to superficial projection neurons, with ~40% of dDH and dTNC projection neurons expressing *Cck* compared to ~10% of superficial projection neurons (**Fig. 3.3A, E**). By contrast, the percentage of *Nptx2* projection neurons is greater in sDH and sTNC (**Fig. 3.3B, F**).

Specifically, in the dorsal horn, *Nptx2* is expressed by 28% of sDH and 13% of dDH projection neurons **(Fig. 3.3B)**. In the TNC the difference is less pronounced, with 32% of sTNC projection neurons expressing *Nptx2* compared to 27% in deeper laminae of the TNC **(Fig. 3.3F)**. *Nmb+* projection neurons are expressed more evenly across superficial and deep laminae, with ~20% of sDH and sTNC projection neurons expressing *Nmb*, compared to 29% in the dDH and 26% in the dTNC **(Fig. 3.3C, G)**. In the dorsal horn, there are 14% of sDH projection neurons that express *Crh* compared with 24% of those in dDH, and in the TNC, 16% of sTNC projection neurons express the gene compared with 7% of dTNC projection neurons **(Fig. 3.3D, H)**. These results not only demonstrate that projection neurons are molecularly diverse but that different populations are distributed in superficial and deep dorsal horn.

Enriched genes define subpopulations of NK1R-positive and negative neurons:

We next performed double fluorescent ISH for these enriched genes and *Tacr1* so as to determine the extent to which these projection neuron markers constitute subsets of the NK1R-expressing projection neurons, or whether they define unique populations (**Fig. 3.4**). In fact, based on their molecular expression pattern, for each gene tested, we observed subpopulations, namely cells that co-expressed the enriched gene and *Tacr1*, as well as cells that singly expressed the gene or Tacr1. Interestingly, we observed *Tacr1*-expressing neurons that co-expressed *Cck* in the deep dorsal horn, but only rarely did we find *Cck* and *Tacr1* coexpressed in neurons in lamina I (**Fig. 3.4A**). In both superficial and deep dorsal horn, we observed subsets of *Tacr1*-expressing neurons

that coexpress *Nptx2* (**Fig. 3.4B**), *Nmb* (**Fig. 3.4C**), and *Crh* (**Fig. 3.4D**). Whether and to

what extent these subsets of *Tacr1*-expressing neurons overlap is the topic of ongoing

experiments. In all cases, we observed many neurons that solely expressed *Tacr1*, or

that were positive for the marker gene, and not *Tacr1* (**Fig. 3.4A-D**).

Recently, several studies reported that substance P (*Tac1*), which targets the NK1R, is

somewhat unexpectedly expressed by a subset of the NK1R-expressing projection

neurons (Cameron et al., 2015; Huang et al., 2019). We confirmed that report by

demonstrating that *Tac1* mRNA is co-expressed with *Tacr1* in a subset of projection

neurons labeled with retrobeads (**Supplemental Fig**. **3.3**). As to other potentials

markers of projection neurons, Häring et al. (2018) delineated several genes that cluster

with *Tacr1* in the dorsal spinal cord, including *Lypd1* and *Elavl4*. Our RNA-seq data

confirm those observations, and we also demonstrate by ISH that these genes co-occur

in many *Tacr1*-expressing spinoparabrachial neurons (**Supplemental Fig. 3.4**).

Molecular heterogeneity of the NK1R-expressing dorsal horn neurons:

We also investigated whether the genes in question define non-overlapping

subpopulations or whether distinct subpopulations can be distinguished based on

varying enriched-gene expression combinations. Here we used triple fluorescent ISH

and observed neuron subtypes that express every combination of the genes (**Fig.

3.5A**). Specifically, some neurons triple-label for *Tacr1, Cck, and Nptx2* (**Fig. 3.5A, 1**);

others coexpress two of these genes (**Fig. 3.5A, 2-4**), and a number only express one

of the

three (**Fig. 3.5A, 5-7**). Based on this result, we conclude that there are at least 4 subsets of *Tacr1*-expressing neurons: *Tacr1+Cck+Nptx2+* **(Fig. 3.5A1)***, Tacr1+Cck +Nptx2-* **(Fig. 3.5A4)***, Tacr1+Cck-Nptx2+* **(Fig. 3.5A2)***, and Tacr+Cck-Nptx2-* cells **(Fig. 3.5A7)**. Assuming that many *Tacr1+* neurons are projection neurons, it follows that there are molecular distinct subpopulations of dorsal horn projection neurons.

Pain and itch-provoking stimuli engage subsets of molecularly-defined projection neurons:

We next used *Fos* expression to determine whether the subsets of projection neurons that express one of the enriched genes are activated by algogenic (painful) or pruritic (itch-provoking) stimuli. These studies were performed in mice that were injected with retrobeads into the LPb two weeks prior to stimulation in order to identify projection neurons. Under isoflurane anesthesia a noxious heat stimulus was produced by submerging the hindpaw in 50C water for 30s. For the pruritic stimulus, we injected chloroquine (500μg) into the cheek. Twenty minutes after either stimulus the animals were euthanized and tissue prepared by ISH for pain or itch-induced *Fos* and one of the enriched genes (**Figs. 3.6 and 3.7**) in the lumbar spinal cord and TNC, respectively.

As expected *Fos* induction was more pronounced ipsilateral to the stimulation, compared to the contralateral side. **Supplemental Figure 3.5** shows the typical pattern of heat evoked Fos immunoreactivity, with the greatest number of *Fos+* neurons in superficial laminae (I/II) of the lumbar dorsal horn. Although *Cck+* projection neuron

expression predominates in laminae III/IV (**Fig 3.3A, E**), we observed *Fos* and *Cck*-positive projection neurons in both lamina I and III/IV (**Fig. 3.6A**). On average, about 33% of all projection neurons in lumbar cord were *Cck*-positive, and 9% expressed *Cck* and were noxious-heat responsive (**Fig. 3.6B**) indicating that ~27% of *Cck*-projection neurons responded to noxious heat. For the *Nptx2* population, we observed 41% of projection neurons that were *Nptx2+* and 21% that expressed *Nptx2* and *Fos* after noxious heat stimulation (**Fig. 3.6C,D**), suggesting that roughly 50% of *Nptx2*-expressing projection neurons respond to painful heat stimulation. *Nmb* (**Fig. 3.6E, F**) and *Crh* (**Fig. 3.6G, H**) both have highly restricted expression, with only a few positive cells per section. We observed 36% of projection neurons that were *Nmb*-positive and 10% that were both *Nmb* and *Fos* expressing, indicating that 27% of *Nmb+* projection neurons are "pain" responsive. Finally, for the *Crh* population, we recorded 26% of projection neurons expressing the gene, and 12% of projection neurons that expressed *Crh* and responded to noxious heat, suggesting that roughly 50% of *Crh*-positive projection neurons respond to noxious heat.

As for our findings after noxious heat stimulation, we observed subsets of chloroquine-responsive projection neurons positive for each of the above enriched genes (**Fig. 3.7**). *Cck* positive neurons comprised 24% of the entire projection neuron population in the TNC, while those that expressed *Cck* and *Fos* after pruritic stimulation only comprise 7%. This indicates that 29% of *Cck+* projection neurons are activated by pruritic stimulation. We found 33% of TNC projection neurons express *Nptx2*, while 12% express both *Nptx2* and *Fos*, suggesting that ~36% of *Nptx2* positive projection

neurons in the TNC respond to chloroquine stimulation. As for the *Nmb* population, we counted 25% of projection neurons that express *Nmb*, 8% that express *Nmb* and *Fos*, which means that 32% of *Nmb*-expressing projection neurons are "itch" responsive. Lastly, we found only 14% of the projection neurons in the TNC express *Crh*, and 4% that express the gene and *Fos*, indicating that 28% of *Crh* positive projection neurons respond to the pruritic stimulation. To summarize, we report here that there are subsets of projection neurons, defined by the enriched genes, that respond to pain-provoking stimulation as well as subsets that respond to itch-provoking stimulation.

DISCUSSION

Summary

There is general agreement that primary sensory neurons and dorsal horn interneurons are heterogeneous, responding selectively to pain and or itch provoking stimuli. On the other hand, despite considerable evidence that the projection neurons that transmit pain and itch are diverse in regards to location, projection targets, morphology, and electrophysiological properties, reference is often made to their being a functionally and certainly molecularly homogenous population. We suggest that this focus reflects the fact that the literature tends to limit its scope of projection neurons to those residing in lamina I, those expressing NK1R, and those projecting to the LPb. As the brain generates functionally distinct percepts based on the information transmitted by the projection neurons, not by primary sensory neurons or dorsal horn interneurons, understanding projection neuron diversity is critical. Unfortunately, until recently the resolution of the molecular profiles of projection neurons has been low. Based on the present ribosomal profiling of the spinoparabrachial projection neurons we conclude that there are molecularly distinct subpopulations of projection neurons. These subpopulations can be distinguished based on gene expression, spatial location in the dorsal horn, and responsiveness to pain and/or itch-provoking stimulation.

The NK1R is not the ideal projection neuron marker

A common trend in the literature is to equate "pain" and "itch" projection neurons with NK1R expression. Although Todd and colleagues determined that 80% and ~90% of

lamina I projection neurons in the rat and mouse, respectively, express the NK1R, less than half of deep dorsal horn projection neurons express the receptor. And most importantly, there is only rare mention of the non-NK1R projection neurons, regardless of laminar location (Marshall et al., 1996; Todd et al., 2000; Puskár et al., 2001; Polgár et al., 2008; Cameron et al., 2015). Furthermore, often overlooked is the report that while projection neurons only comprise 5% of all lamina I neurons in lumbar cord (Todd, 2010), up to 45% of all lamina I neurons express the NK1R (Todd et al., 1998). If indeed most lamina I projection neurons express the NK1R, it follows that a very large percentage of NK1R-expressing neurons in lamina I are, in fact, interneurons. Of course, as these counts were of spinoparabrachial projection neurons, the numbers may vary if other NK1R-expressing neurons in lamina I are propriospinal (i.e. project to other spinal cord levels) or target other brainstem regions.

Most importantly perhaps, because NK1R expression does not distinguish subsets of lamina I spinoparabrachial neurons, the receptor is not an ideal marker to interrogate the functional specificity of projection neurons. For example, important papers of Mantyh et al. (1997) and Carstens et al. (2010) found that ablating NK1R-expressing neurons reduces both behaviors indicative of pain and itch. Based on the present findings, however, it is clear that there are several subpopulations of NK1R expressing neurons (**Figs. 3.4 and 3.5**). Because these subpopulations of NK1R-expressing population may transmit modality specific information to the brain, it cannot be concluded that algogenic and pruritic stimuli, either directly or indirectly, converge on the same population of NK1R projection neurons. To address this question, our ongoing studies

are using a highly multiplexed ISH approach, which combines ISH profiling of several

genes in retrogradely labeled projection neurons with pain- or itch-induced *Fos*

expression.

The discrepancy between NK1R mRNA signal, as visualized by ISH, and its protein

level detected by IHC, raises some concern. Consistently, we detect significantly

greater numbers of neurons expressing a given message than is observed by

immunohistochemical demonstration of protein. This is particularly true for the NK1R.

This difference between mRNA and detectable protein could either be due to increased

sensitivity of the ISH compared to immunohistochemistry or it could reflect a real

difference between the rates of gene transcription and translation. We are approaching

this problem by ablating the NK1R-expressing projection neurons after intrathecal

injection of substance P-conjugated saporin (SP-SAP, as described in Mantyh et al.)

and then performing ISH on tissue from these animals. As effective SP-SAP killing of

neurons can only occur if receptor is expressed on the surface of cells, allowing for

internalization of the saporin, persistence of *Tacr1* mRNA signal would argue that the

TacR1 positive cells defined by ISH do not, in fact, synthesize protein. Alternatively, if

ablation of the protein-expressing cells also leads to the disappearance of the mRNA

signal, we can be confident that the ISH method is detecting signal that indeed reflects

neurons that express functional NK1R.

Häring et al. (2018) and Sathyamurthy et al. (2018) recently reported on the molecular

heterogeneity of spinal cord neurons using single-cell or single-nucleus RNA

sequencing. Sathyamurthy et al. identified 16 dorsal excitatory neuron types, but

interestingly, they concluded that none are defined uniquely by NK1R expression, and

they made no mention of projection neurons, which were not segregated or profiled

independently of the entire neuronal population. In contrast, Häring et al. delineated 15

dorsal excitatory neuron categories and, by integrating a retrograde tracing approach

into their ISH confirmation analyses, concluded that spinoparabrachial neurons are

concentrated within one of 15 clusters of excitatory neurons (Glut 15). Our study differs

considerably from these studies in approach, experimental procedures, and most

importantly, in conclusions. Here we used bulk profiling of isolated projection neuron

ribosomes from dorsal spinal cord and TNC tissue to illustrate the molecular

heterogeneity of projection neurons. We certainly and not surprisingly concur with

Häring et al.'s identification of Glut 15 (one of the clusters defined by NK1R enrichment)

as a projection neuron population (e.g. we identified _Crh_ in projection neurons and _Crh_

is included in the Glut 15 cluster; also see **Supplementary Fig. 3.4**). On the other

hand, our results indicate that there are projection neurons that are members of

excitatory populations other than Glut15. For example, the fact that we identified _Cck+,_

Nptx2+ and _Nmb+_ projection neurons demonstrates that there are spinoparabrachial

neurons within the excitatory clusters Glut 2, 3, 7, 9, and 11-14.

Interestingly, Häring et al. focused solely on *Lypd1* as a novel marker for projection neurons. We certainly agree that Lypd1 is a general marker gene, comparable to *Tacr1* in its ability to label a large percentage of all projection neurons, but not able to define subtypes. Our study reveals several additional marker genes for dorsal horn projection neurons that have a restricted expression pattern and define discrete subtypes.

Specificity versus convergence and the generation of pain and itch percepts

To what extent molecularly-defined subpopulations of projection neurons are specific for a given pain modality or for itch remains an unanswered question. Studies in which cell-type specific ablation or stimulation (e.g. using DREADDS, genetic knockouts or optogenetically) have been performed suggests that pain and itch are transmitted along labeled-lines, at least at the level of the primary afferent or the interneurons (Sun and Chen, 2007; Cavanaugh et al., 2009; Liu et al., 2009; Sun et al., 2009; Knowlton et al., 2013; Duan et al., 2014). However, electrophysiological data overwhelmingly suggest polymodality at all levels of the neuraxis, implying that pain and itch either converge on modality-indiscriminate circuits, or that a population code is in effect, such that labeled-lines exist but that there is cross talk between the different lines (Ma, 2012). Our *Fos* studies (**Figs. 3.6 and 3.7**) suggest that each dorsal horn population of *Cck-*, *Nptx2-*, *Crh-*, and *Nmb*-expressing projection neurons includes a subset that is activated by noxious heat, as well as a subset that is activated by pruritic stimulation. However, we cannot conclude from these data whether and to what extent there is convergence of modalities, i.e. the same subset responds to noxious heat and pruritic stimulation, which is suggested from several electrophysiological studies. However, these polymodal

projection neuron subpopulations may nevertheless transmit modality specific

information based on a population code generated across projection neurons. To

answer that question will require a functional analysis of the consequence of activity of

the population code using, for example, cell-specific ablation or stimulation. The

neuroanatomical analysis reported here taken together with the RNASeq identification

of enriched projection neuron genes should greatly facilitate future studies into how the

brain interprets algogenic and prurtitic inputs so as to produce pain vs itch percepts.

METHODS

Animals

Animal experiments were approved by the UCSF Institutional Animal Care and Use

Committee and were conducted in accordance with the NIH Guide for the Care and Use

of Laboratory animals. We used male and female wild type C57BL/6J mice (Jackson

Laboratory, Stock #000664) and transgenic mice that express Cre-recombinase in

NK1R-expressing neurons (gift from Dr. Xinzhong Dong, Baltimore, USA). All mice used

were between 6-12 weeks of age and were housed on a 12 hr light-dark schedule.

Stereotaxic Injections

To tag ribosomes of projection neurons in the spinal cord dorsal horn and trigeminal

nucleus caudalis (TNC) for immunoprecipitation, we first anesthetized adult mice with

ketamine (60 mg/kg)/xylazine (8.0 mg/kg). Mice were mounted in a stereotaxic frame

and injected with i.p. Carprofen (0.1mg/kg, Rymadyl). We shaved the top of the head,

disinfected the area with alcohol swabs and Povidone-iodine, and applied protective

ointment on the eyes. We applied 0.5% topical Lidocaine on the scalp, and tested for

loss of nociceptive withdrawal reflex before making an incision along the midline of the

scalp. The skull was cleaned and 3% hydrogen peroxide was used to visualize bregma.

Bilateral craniotomies were made with a microdrill above the lateral parabrachial

nucleus (LPb, coordinates: ±1.3 mm from midline, -5.34 mm from Bregma, -3.6 mm

from skull) and we injected bilaterally 0.5μl of a retrograde herpes simplex-based viral

vector expressing the large ribosomal subunit protein L10a (gift from Dr. Zachary Knight, UCSF). In the wild type mice, we used a viral vector that expresses a GFP-tagged L10a (HSV-hEF1a-GFP-L10a) and in the NK1R-Cre mice we used a viral vector that expresses Cre recombinase-dependent HA-tagged L10a (HSV-hEF1a-LS1L-Flag-HA-L10a). After each viral injection, the needle was left in place for 5 minutes before slowly retracting. The skin was then sutured and the mice were returned to their cages, given post-op analgesic buprinorphine-SR (0.15mg/kg, i.p.) and monitored for recovery. Mice were killed 2-3 weeks after surgery and their tissue dissected for immunoprecipitation.

To retrogradely label projection neurons of the spinal cord dorsal horn and TNC that could subsequently be studied by ISH, we followed the above surgical procedures. However, in these studies wild type mice received either: unilateral or bilateral injections of 0.5 µl of green Retrobeads (Lumafluor), or HSV-hEF1a-GFP-L10a, into the LPb.

Immunoprecipitation, RNA and cDNA preparation

To immunoprecipitate tagged ribosomes and their associated mRNA, we followed the protocol described by Ekstrand et al. (2014), with minor modifications. Protein A Dynabeads (100 µl per IP, Invitrogen) were washed twice on a magnetic rack with Buffer A (10 mM HEPES [pH 7.4], 150 mM KCl, 5 mM MgCl2, 1% NP40). After the final wash, the beads were resuspended in Buffer A with 0.1% BSA and loaded with either anti-GFP polyclonal antibody (25 µg per IP, abcam) or anti-HA-tag monoclonal antibody (2 µg per IP, Cell Signaling). Antibody-bead conjugates were mixed at 4℃ overnight.

Mice were killed with an overdose of 1X Avertin and dorsal spinal cord and TNC were rapidly dissected in ice-cold Buffer B (1xHBSS, 4 mM NaHCO3, 2.5 mM HEPES [pH 7.4], 35 mM Glucose) with 100 µg/ml cycloheximide (Sigma). The dissected pieces were pooled in 2 groups of 4 mice each (1 group of injected experimental mice, 1 group of non-injected controls), transferred to a glass homogenizer (Kimble Kontes 20), and homogenized in 1.5 ml ice-cold Buffer C (10 mM HEPES [pH 7.4], 150 mM KCl, 5 mM MgCl2) with 0.5 mM DTT (Sigma), 20 U/µl Superase-In (Invitrogen), 100 µg/ml cycloheximide, and protease inhibitor cocktail (Roche). Tissue samples were homogenized 3 times at 300 rpm and 10 times at 800 rpm on a variable-speed homogenizer (Glas-Col) at 4°C. Homogenates were transferred to microcentrifuge tubes and clarified at 2,000xg for 10 min at 4°C. 10% IGEPAL CA-630 (NP-40; Sigma) and 1,2-diheptanoyl-sn-glycero-3-phospho-choline (DHPC at 100 mg/0.69 ml; Avanti Polar Lipids) were then added to the supernatant for a final concentration of 30mM and 1%, respectively. The solutions were mixed and centrifuged again at 20,000xg for 15 min at 4°C. The resulting supernatants were transferred to new tubes and 50 µl of each cleared lysate was mixed with 50 µl Lysis Buffer (0.7 µl β-mercaptoethanol/100 µl Lysis Buffer; Agilent Absolutely RNA Nanoprep Kit) and stored at −80° for later preparation as Input RNA. The remaining lysates (approximately 1.5 ml) were used for immunoprecipitation. The beads incubating with GFP or HA antibodies were washed twice in Buffer A before the tissue lysates were added. The GFP and HA IPs were allowed to run at 4°C for 5 or 10 min, respectively. Beads were washed 4 times with Buffer D (10 mM HEPES [pH 7.4], 350 mM KCl, 5 mM MgCl2, 1% NP40) with 0.5 mM DTT, 20 U/µl Superase-In Plus and 100 µg/ml cycloheximide. Before removing the last

wash solution the beads were transferred to a new tube. After the final wash, RNA was eluted by adding 100 µl Lysis Buffer and purified using the Absolutely RNA Nanoprep Kit (Agilent). cDNA was prepared with the Ovation RNA-seq V2 kit (Nugen) and a portion was set aside for analysis with Taqman qPCR (see below for methods). Libraries for RNA-seq were prepared with the remaining cDNA using the Ovation Ultralow Library System (NuGen).

RNA Yield and Quality

RNA yield (ng/µl) and quality (RIN value) were quantified using an Agilent 2100 Bioanalyzer and the Agilent RNA 6000 Pico Kit (Cat No. 5067-1513). IP RNA yields for the GFP IP ranged from 0.1-0.9 ng/µl and yields from the HA IP ranged from 2.5-3.5 ng/µl. Input RNA yield ranged from 50-90 ng/µl. We only analyzed samples with RIN values of 8.4 or greater.

Quantitative PCR

Dorsal spinal cord and TNC tissue were homogenized, and RNA and cDNA were prepared as described above. mRNA levels were quantified with the Bio-Rad CFX Connect System using TaqMan Gene Expression Assay (Applied Biosystems). Taqman data analysis and statistics were performed using Microsoft Excel. All Taqman values were normalized to ribosomal protein Rpl27. Fold enrichment plots from Taqman data were obtained by dividing the IP RNA value for each gene by the Input RNA value (IP/Input). A paired Student's t test was performed to compare IP and Input RNA.

Sequencing and Bioinformatic Analysis

RNA-Sequencing was performed on an Illumina HiSeq 4000 sequencer using 50 bp single-end reads. For the GFP-IP experiment, 8 samples were sequenced: 4 Immunoprecipitate replicates paired with 4 Input replicates, which were obtained from pooling 4 mice per replicate. For the HA-IP experiment, 6 samples were sequenced: 3 Immunoprecipitate replicates paired with 3 Input replicates, which again were obtained from pooling 4 mice per replicate. RNA-seq data were processed in Galaxy and further analyzed with Microsoft Excel and MATLAB (R2015b). RNA STAR (v 2.6.0b) was used to align the reads. Htseq-count (v 0.9.1) and DESeq2 (v 1.18.1) were used for transcript abundance estimation and differential expression testing, respectively. The UCSC GRCm38 (mm10 build) was used for gene annotation.

In Situ Hybridization (ISH)

To detect and confirm expression of marker genes in spinal cord and TNC tissue we performed fluorescent in situ hybridization (ISH) using the RNAscope Multiplex Fluorescent Assay (Advanced Cell Diagnostics, cat no. 320850) and target probes. For the complete list of probes used, see Supplementary Table 1. For these experiments, we perfused adult C57BL/6J mice with room temperature 1X PBS. The TNC and spinal cord were rapidly dissected out, frozen on dry ice, and kept at -80℃. From these tissues, we cut 12µm cryostat sections and stored the sections at -80℃ until use.

For *Fos* induction studies: Mice were injected two weeks prior to stimulation with HSV-hEF1a-GFP-L10a or green retrobeads (Lumafluor) into the LPb, to label

spinoparabrachial neurons. For pruritic stimulation, we injected 500μg in 100μL chloroquine (CQ) into the left cheek, and performed ISH in the TNC for *Fos*, and each marker gene. In mice in which projection neurons were labeled with HSV-hEF1a-GFP-L10a we also used a *Gfp* probe.

Sensory stimulation for ISH

All mice were injected i.p. with an anesthetizing dose of avertin (1.25%) 20-30 minutes before stimulation and killed 15-30 min after stimulation. For noxious heat stimulation, we submerged the left hindpaw in 50°C water for 30s and performed ISH on lumbar spinal cord.

Imaging & Image Analysis

All images were taken with an LSM 700 confocal microscope (Zeiss) equipped with 405-nm (5mW fiber output), 488-nm (10mW fiber output), 55-nm (10-mW fiber output), and 639-nm (5-mW fiber output) diode lasers using a 20x Plan Apochromat (20x/0.8) objective (Zeiss). Image acquisition was done with Zeiss Zen software (2010). The same imagine parameters were used for all images within an experiment.

For quantitative analysis of transcript expression, we analyzed 12μm sections from 2-4 animals per condition (3-6 sections per animal). Since we performed the pruritic stimulation in the cheek (to allow for a larger chloroquine volume), we analyzed TNC tissue in these experiments. For the noxious heat stimulation experiments, we analyzed lumbar spinal cord (L3-5). We used a custom MATLAB script to count cells positive for

the retrograde-label (retrobeads or GFP) and subsequently determined the percentage of these cells that were positive for the marker genes and/or *Fos*. For quantitative analysis of the spatial distribution of enriched genes, we used MATLAB to manually draw a border between superficial and deep dorsal horn or TNC and used a custom MATLAB script to count the percentage of projection neurons in each region that express each gene. To calculate the final percentages of gene expression and spatial distribution, we averaged counts and percentages across sections in each animal, and again across animals per experimental group.

Supplementary Table : List of ISH probes used

Probe Name	Cat No.	Channel
RNAscope® Probe- Mm-Cck	402271	C1
RNAscope® Probe- Mm-Crh	316091	C1
RNAscope® Probe- Mm-Fos	316921	C1
RNAscope® Probe- Mm-Lypd1	318361	C1
RNAscope® Probe- Mm-Nmb	459931	C1
RNAscope® Probe- Mm-Nptx2	316901	C1
RNAscope® Probe- Mm-Tac1	410351	C1
RNAscope® Probe- Mm-Tacr1	428781	C1
RNAscope® Probe- Mm-Cck	402271-C2	C2
RNAscope® Probe- Mm-Crh	316091-C2	C2
RNAscope® Probe- Mm-Elavl4	479581-C2	C2
RNAscope® Probe- Mm-Fos	316921-C2	C2
RNAscope® Probe- Mm-Gfp	409011-C2	C2
RNAscope® Probe- Mm-Nmb	459931-C2	C2
RNAscope® Probe- Mm-Tacr1	428781-C2	C2
RNAscope® Probe- Mm-Fos	316921-C3	C3
RNAscope® Probe- Mm-Gfp	409011-C3	C3
RNAscope® Probe- Mm-Lypd1	318361-C3	C3
RNAscope® Probe- Mm-Tacr1	428781-C3	C3

Not published

RNAscope® Probe- Mm-Sprr1a	426871	C1
RNAscope® Probe- Mm-Vip	415961	C1
RNAscope® Probe- Mm-Grpr	317871	C2
RNAscope® Probe- Mm-Cartpt	432001-C3	C3

From Q4

RNAscope® Probe- Mm-Casc4	435101	C1
RNAscope® Probe- Mm-Cdk16	423781	C1
RNAscope® Probe- Mm-Egr3	431101	C1
RNAscope® Probe- Mm-Lynx1	449071	C1
RNAscope® Probe- Mm-Mgat5	523961	C1
RNAscope® Probe- Mm-Neto2	434141	C1
RNAscope® Probe- Mm-Rnf10	496251	C1
RNAscope® Probe- Mm-Vegfb-CDS	424301	C1
RNAscope® Probe- Mm-Kcnh5	497691-C2	C2
RNAscope® Probe- Mm-Thra	519421-C2	C2
RNAscope® Probe- Mm-Tmtc1	518221-C2	C2
RNAscope® Probe- Mm-Cux2	469551-C3	C3
RNAscope® Probe- Mm-Gsg1l	478551-C3	C3
RNAscope® Probe- Mm-Necab3	428561-C3	C3

Supplementary Table 3.2: Genes significantly enriched in the PN dataset and significantly depleted in the NK dataset, suggestive of molecular markers for the nonNK1R-expressing population of projection neurons

GeneID	log_FC	StdErr	Pvalue	PAdj	Sample
Dok6	1.010987774	0.369096342	0.006160967	0.036703431	PN_IP_V_Input
Dok6	-1.321410083	0.46073848	0.004130412	0.024215917	NK_IP_V_Input
Mospd3	0.756329408	0.241056715	0.001703616	0.013693147	PN_IP_V_Input
Mospd3	-1.434792519	0.26133244	4.0126E-08	1.07377E-06	NK_IP_V_Input
Cux2	1.002199362	0.300920978	0.000867087	0.007989666	PN_IP_V_Input
Cux2	-1.048079831	0.327702063	0.001382545	0.010027471	NK_IP_V_Input
Dynll2	1.292090251	0.187623613	5.71384E-12	8.14117E-10	PN_IP_V_Input
Dynll2	-0.548868532	0.135335215	5.0001E-05	0.000614225	NK_IP_V_Input
Vegfb	0.720931173	0.263976823	0.006313487	0.037323067	PN_IP_V_Input
Vegfb	-1.187602461	0.231332781	2.8404E-07	6.37598E-06	NK_IP_V_Input
Igf2bp3	1.09225678	0.289677667	0.00016286	0.002105953	PN_IP_V_Input
Igf2bp3	-0.81663896	0.302830962	0.007003401	0.036825094	NK_IP_V_Input
Trappc3	0.73363012	0.218919765	0.000804805	0.007551425	PN_IP_V_Input
Trappc3	-0.884416651	0.196743904	6.94823E-06	0.000109273	NK_IP_V_Input
1810037I17Rik	0.762069848	0.256014276	0.002913981	0.020836589	PN_IP_V_Input
1810037I17Rik	-0.853543311	0.300856113	0.004553273	0.026193072	NK_IP_V_Input
C330006A16Rik	0.531209302	0.172542502	0.00207895	0.015971485	PN_IP_V_Input
C330006A16Rik	-0.971618037	0.158412451	8.59826E-10	3.15627E-08	NK_IP_V_Input
B230217C12Rik	0.9281773	0.172929543	7.98919E-08	3.33164E-06	PN_IP_V_Input
B230217C12Rik	-0.588274362	0.151250563	0.000100491	0.001114646	NK_IP_V_Input
Nipal3	0.673967795	0.236130868	0.004314359	0.028071611	PN_IP_V_Input
Nipal3	-0.838695372	0.239891799	0.000472041	0.00410049	NK_IP_V_Input
Guk1	0.792790984	0.289419743	0.006158085	0.036700471	PN_IP_V_Input
Guk1	-0.725431385	0.205987237	0.000428741	0.003802608	NK_IP_V_Input
Gsg1l	0.722384976	0.230316085	0.00170981	0.013732027	PN_IP_V_Input
Gsg1l	-0.743052068	0.242220486	0.00215736	0.014371042	NK_IP_V_Input
Edf1	0.866973505	0.28744882	0.002560514	0.018709016	PN_IP_V_Input
Edf1	-0.460591321	0.177715782	0.009549469	0.047101254	NK_IP_V_Input
Nsun3	0.700080516	0.249017993	0.004933176	0.030997024	PN_IP_V_Input
Nsun3	-0.685796889	0.249740311	0.00603194	0.032754717	NK_IP_V_Input
Thra	0.624222913	0.189774797	0.001004432	0.009017616	PN_IP_V_Input
Thra	-0.721886019	0.190668279	0.00015304	0.001599184	NK_IP_V_Input
Rcan3	0.571483903	0.175549808	0.001132349	0.009907768	PN_IP_V_Input
Rcan3	-0.719796665	0.174172283	3.58573E-05	0.000458532	NK_IP_V_Input
Sod1	0.801803237	0.255680614	0.001712947	0.013750042	PN_IP_V_Input
Sod1	-0.416128328	0.138875849	0.002731831	0.017353133	NK_IP_V_Input
Uhmk1	0.526825021	0.174198176	0.002492211	0.018305558	PN_IP_V_Input
Uhmk1	-0.731897157	0.161613886	5.9354E-06	9.4488E-05	NK_IP_V_Input
Casc4	0.771003276	0.227604965	0.000705424	0.006792903	PN_IP_V_Input
Casc4	-0.459189893	0.164757898	0.005318888	0.029699347	NK_IP_V_Input

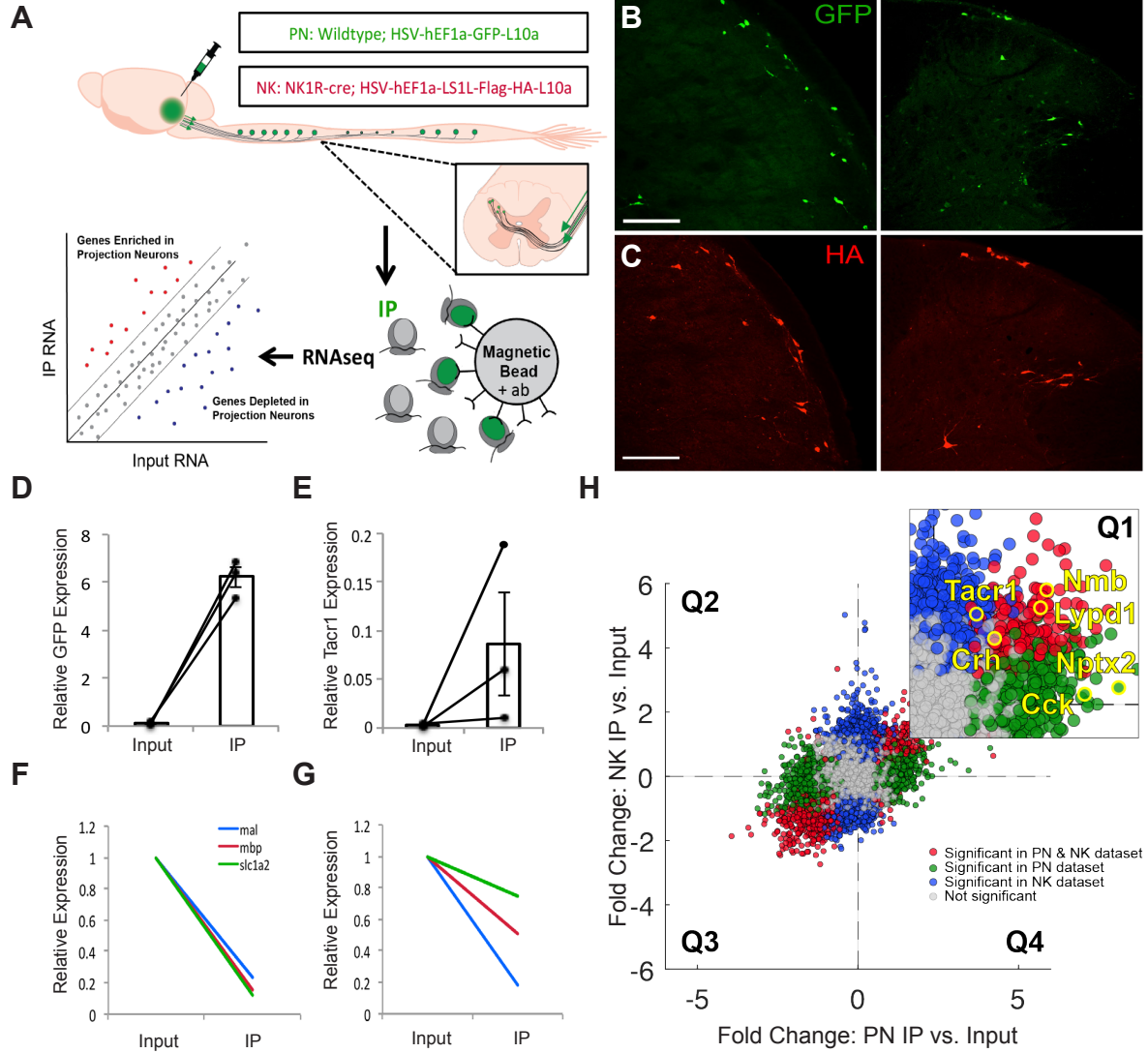| GeneID	log_FC	StdErr	Pvalue	PAdj	Sample
Mlec	0.657695765	0.165261143	6.89918E-05	0.001025744	PN_IP_V_Input
Mlec	-0.610118806	0.162687323	0.000176655	0.001802486	NK_IP_V_Input
Ebag9	0.747897427	0.258644387	0.003832794	0.025665374	PN_IP_V_Input
Ebag9	-0.480328964	0.174535934	0.005922623	0.032295994	NK_IP_V_Input
Necab3	0.635655284	0.237875533	0.007535168	0.042551934	PN_IP_V_Input
Necab3	-0.592142461	0.196663278	0.002604354	0.01672038	NK_IP_V_Input
Sdf4	0.687347899	0.149811475	4.47329E-06	0.000103823	PN_IP_V_Input
Sdf4	-0.509026698	0.127511196	6.5514E-05	0.000770803	NK_IP_V_Input
Rnf220	0.758387116	0.226553504	0.000815449	0.007628047	PN_IP_V_Input
Rnf220	-0.385708888	0.144107356	0.007438702	0.038504043	NK_IP_V_Input
Ube2r2	0.726131528	0.142180791	3.27141E-07	1.13124E-05	PN_IP_V_Input
Ube2r2	-0.423917566	0.125738412	0.000747805	0.00601173	NK_IP_V_Input
Rrm2b	0.482890667	0.171659019	0.004906934	0.030895214	PN_IP_V_Input
Rrm2b	-0.681558089	0.193590773	0.000430551	0.003816495	NK_IP_V_Input
Limk1	0.467905642	0.174053769	0.007182068	0.040965364	PN_IP_V_Input
Limk1	-0.66902982	0.182617546	0.000248737	0.002414071	NK_IP_V_Input
Neto2	0.581102842	0.202669453	0.004140632	0.027229079	PN_IP_V_Input
Neto2	-0.5581333	0.177942609	0.00170924	0.011909716	NK_IP_V_Input
Tmem196	0.626377572	0.17471129	0.0003368	0.003796838	PN_IP_V_Input
Tmem196	-0.484869027	0.173161547	0.005108734	0.028731567	NK_IP_V_Input
Gnal	0.697068188	0.15052535	3.64076E-06	8.65904E-05	PN_IP_V_Input
Gnal	-0.365059991	0.115004477	0.001501926	0.01072873	NK_IP_V_Input
Tmem50b	0.508692279	0.169570044	0.002700729	0.019520349	PN_IP_V_Input
Tmem50b	-0.542103876	0.139110042	9.74146E-05	0.001086709	NK_IP_V_Input
Pgr	0.551527972	0.203333001	0.006679046	0.038754585	PN_IP_V_Input
Pgr	-0.489915993	0.180810849	0.00673746	0.035691378	NK_IP_V_Input
Creg2	0.619533953	0.214526969	0.003878144	0.025901425	PN_IP_V_Input
Creg2	-0.380818583	0.139273613	0.006250932	0.033755899	NK_IP_V_Input
Fam171b	0.526097889	0.199361905	0.008317335	0.045709695	PN_IP_V_Input
Fam171b	-0.495278847	0.150419816	0.000992502	0.007620678	NK_IP_V_Input
Anks1b	0.538552074	0.173713285	0.001933669	0.015073606	PN_IP_V_Input
Anks1b	-0.451095661	0.153435749	0.003282498	0.020153583	NK_IP_V_Input
Hiat1	0.49297395	0.16336363	0.002547445	0.018644979	PN_IP_V_Input
Hiat1	-0.451473625	0.161277195	0.005120333	0.02877605	NK_IP_V_Input
Reep5	0.567509958	0.183089984	0.00193767	0.015097147	PN_IP_V_Input
Reep5	-0.327345986	0.117746364	0.005434313	0.030192275	NK_IP_V_Input
Negr1	0.519674132	0.142231325	0.000258463	0.003090559	PN_IP_V_Input
Negr1	-0.375927579	0.132999424	0.004705454	0.026860517	NK_IP_V_Input

A

PN: Wildtype; HSV-hEF1a-GFP-L10a

NK: NK1R-cre; HSV-hEF1a-LS1L-Flag-HA-L10a

Genes Enriched in Projection Neurons

Genes Depleted in Projection Neurons

IP RNA

Input RNA

RNAseq

IP

Magnetic Bead + ab

B GFP

C HA

D

Relative GFP Expression

Input   IP

E

Relative Tacr1 Expression

Input   IP

F

Relative Expression

— mal
— mbp
— slc1a2

Input   IP

G

Relative Expression

Input   IP

H

Fold Change: NK IP vs. Input

Fold Change: PN IP vs. Input

Q1
Q2
Q3
Q4

Tacr1   Nmb
Crh   Lypd1
Nptx2
Cck

Significant in PN & NK dataset
Significant in PN dataset
Significant in NK dataset
Not significant

Figure 3.1: Selective purification and profiling of projection neurons reveals candidates for projection neuron marker genes

(A) Schematic of experimental design: HSV-GFPL10 (in PN experiments) or HSV-HAL10 (in NK experiments) was injected into LPb of wildtype or NK1R-cre mice to tag ribosomes of spinal and medullary projection neurons for immunoprecipitation and subsequent RNA sequencing. **(B)** Representative images of GFP immunofluorescence in nucleus caudalis (left) and spinal cord (right) from wildtype mice showing projection neurons with GFP-tagged ribosomal protein. Scale bar, 100µm. **(C)** Representative images of HA immunofluorescence in nucleus caudalis (left) and spinal cord (right) from NK1R-Cre mice showing projection neurons with HA-tagged ribosomal protein. Scale bar, 100µm. **(D and E)** qPCR results showing enrichment of Gfp **(D)** and Tacr1 **(E)** in IP relative to Input samples, in PN and NK experiments, respectively. Data are normalized to Rpl27 and represented as mean ± SEM. **(F and G)** qPCR results showing depletion of glial genes in IP relative to Input samples in PN **(F)** and NK **(G)** experiments. Data are normalized to Rpl27 and Input relative expression and represented as mean ± SEM **(H)** RNA sequencing results showing differential expression data of IP relative to Input Fold Change for PN experiments versus NK experiments. Quadrant 1 (Q1) contains genes enriched in both datasets, Q2 contains genes depleted in both, Q3 and Q4 contain genes differentially changed in PN versus NK datasets. Inset shows enlarged Q1 with genes of interest shown in yellow. Genes significantly enriched or depleted in both PN and NK datasets are shown in red. Genes significantly changed in PN, but not NK, dataset are shown in green, while genes significantly changed in NK, but not PN, dataset are shown in blue. P<0.05.
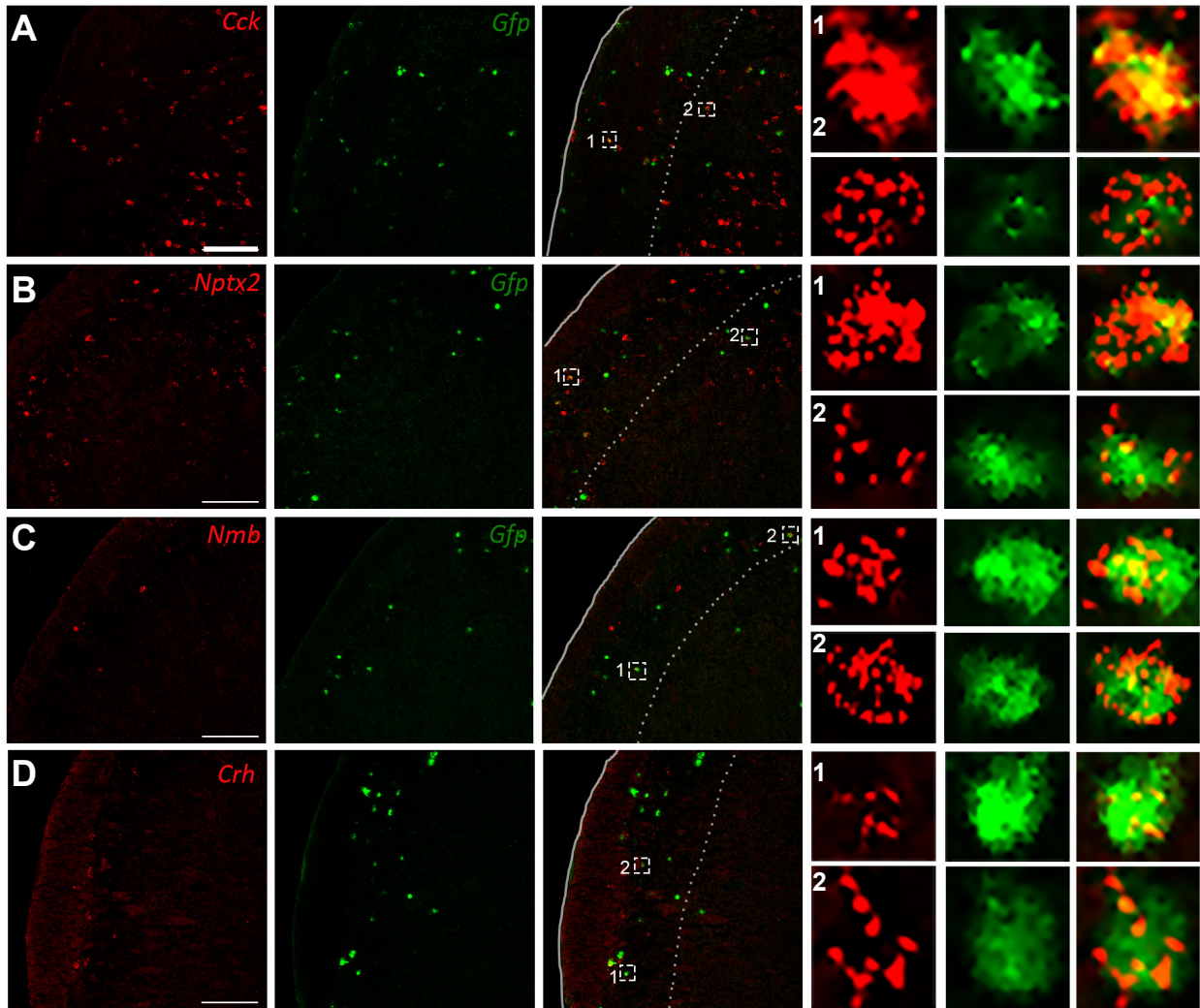
Figure 3.2: RNA sequencing identifies marker genes expressed by projection neurons

Representative TNC sections showing co-labeling of *Cck* **(A)**, *Nptx2* **(B)**, *Nmb* **(C)**, or *Crh* **(D)** mRNA (red) with *Gfp*-tagged spinoparabrachial projection neurons (green). Insets show enlarged examples of individual cells positive for both the marker gene and *Gfp*. Sections are 12μm thick. Scale bars, 100μm.
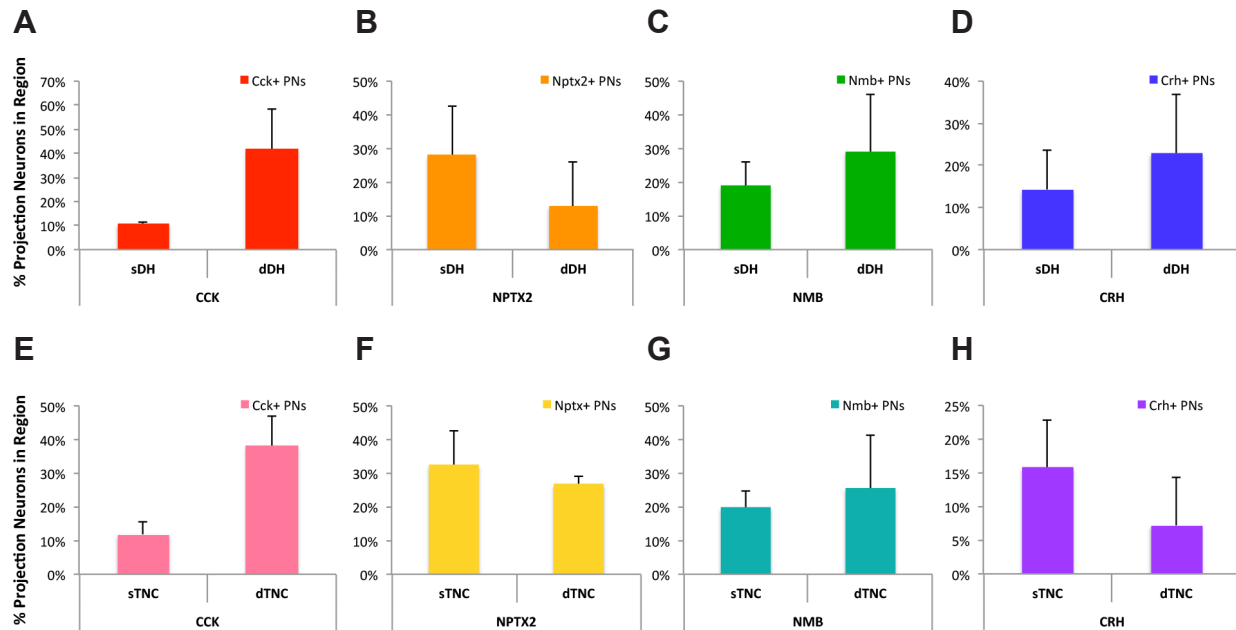
Figure 3.3: Enriched genes are expressed by projection neurons in both superficial and deep dorsal horn:

(A-D) Bar graphs representing the proportion of projection neurons in sDH that express *Cck* **(A)** *Nptx2* **(B)** *Nmb* **(C)** and *Crh* **(D)** compared to the proportion of projection neurons in dDH that express each gene. **(E-F)** Bar graphs representing the proportion of projection neurons in sTNC that express *Cck* **(E)** *Nptx2* **(F)** *Nmb* **(G)** and *Crh* **(H)** compared to the proportion of projection neurons in dTNC that express each gene. sDH, superficial dorsal horn; dDH, deep dorsal horn; sTNC, superficial trigeminal nucleus caudalis; dTNC, deep trigeminal nucleus caudalis; PNs, projection neurons. Data are represented as mean ± SEM.
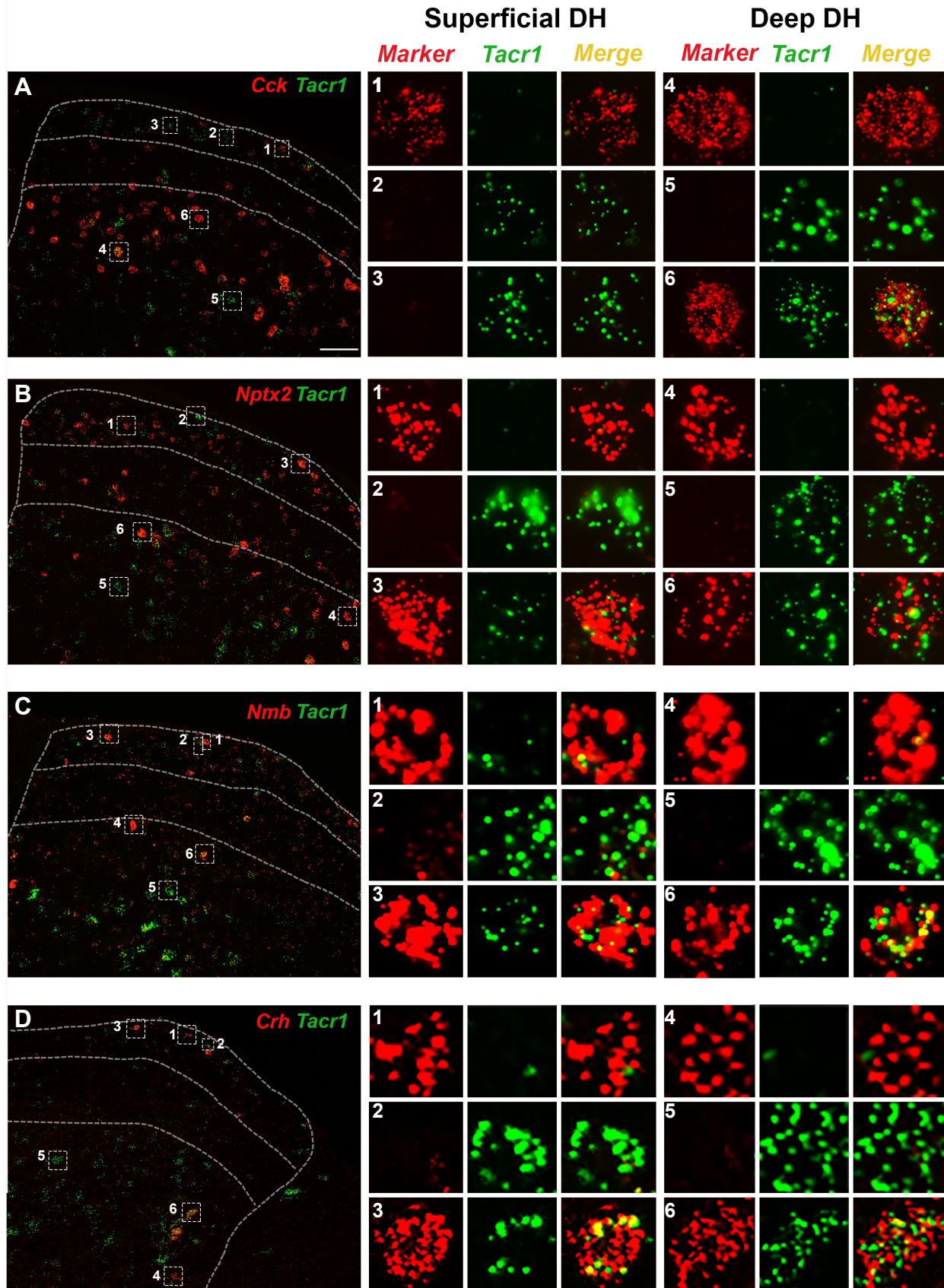
Figure 3.4: Enriched genes are expressed by subpopulations of NK1R-positive and negative neurons

Representative sections from lumbar spinal cord showing expression of *Cck* **(A)**, *Nptx2* **(B)**, *Nmb* **(C)**, or *Crh* **(D)** mRNA (red) with *Tacr1* mRNA (green) in both superficial and deep dorsal horn. Insets show examples of enlarged single-labeled cells for each individual marker gene, or for *Tacr1*, as well as double labeled cells, in superficial (middle panels) and deep (right panels) dorsal horn. Sections are 12µm thick. Scale bars, 100µm.
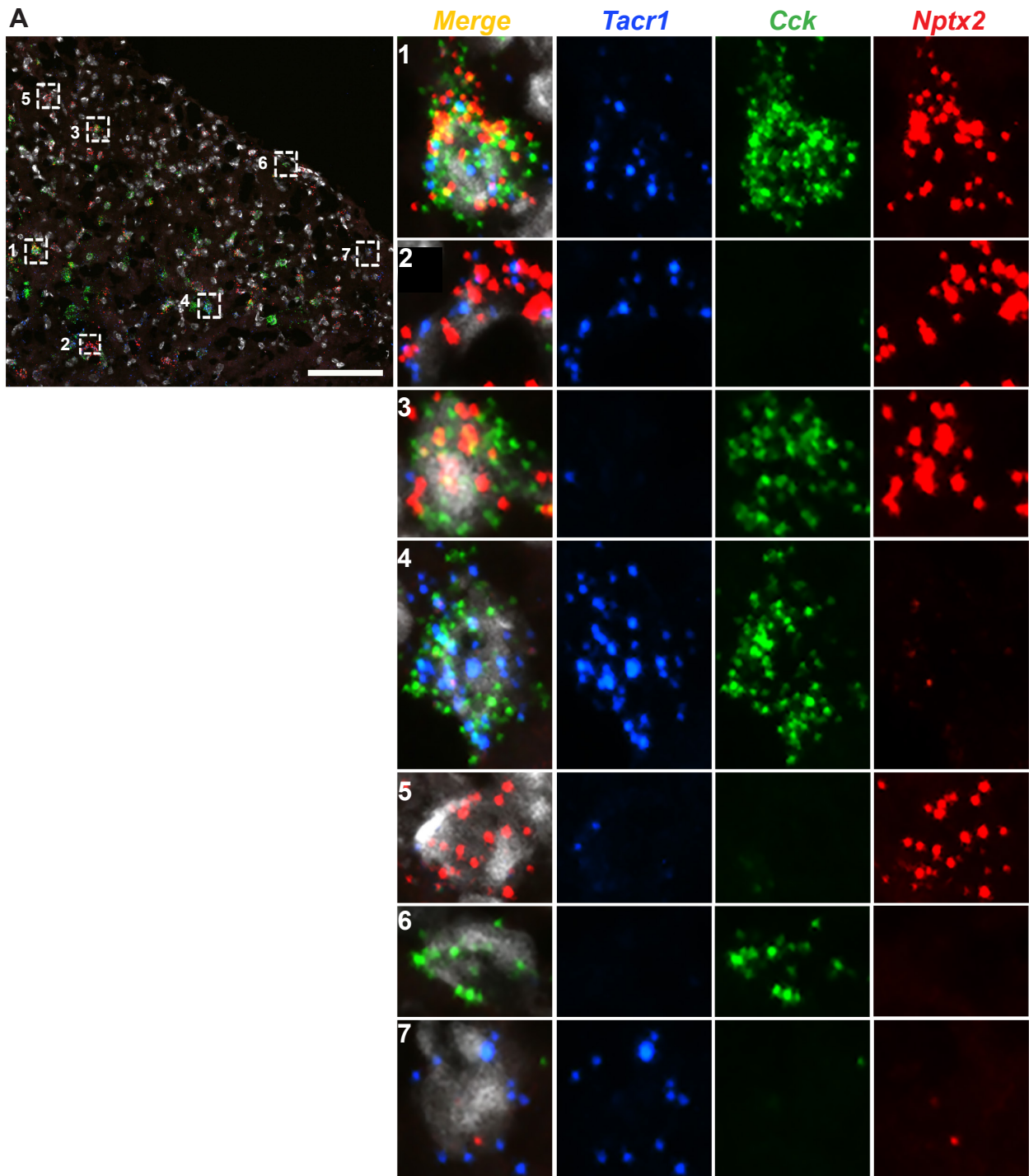
Figure 3.5: Molecular heterogeneity of the NK1R- and nonNK1R-expressing dorsal horn neurons

(A) Representative section (12μm) of lumbar spinal cord after triple ISH for *Tacr1* (blue), *Cck* (green), *Nptx2* (red), and DAPI (white). Insets show examples of enlarged single cells with various combinations of gene expression, including triple labeled **(A,1)**, double labeled **(A, 2-4)**, and single labeled **(A, 5-7)** cells. Scale bar, 100μm. **(B-D)** Automated maps of lumbar dorsal horn showing location of single cells with varying levels of relative co-expression of *Cck* to *Tacr1* **(B)**, *Nptx2* to *Tacr1* **(C)**, and *Cck* to *Nptx2* **(D)**. Relative level of co-expression is visualized by the color scale indicated. Data are averaged over 3 mice, 5 sections per mouse, and are represented as log2 (ratio).
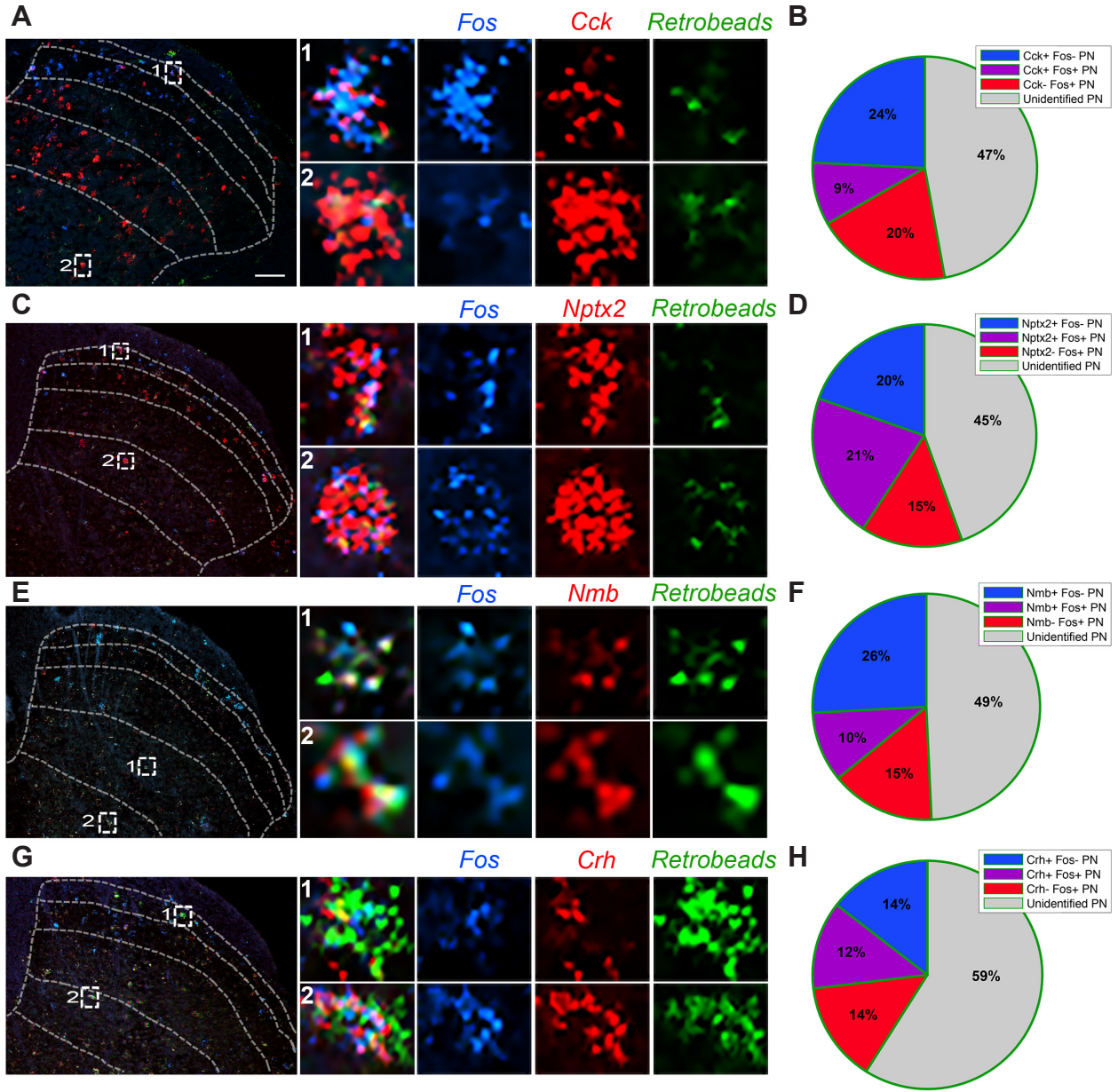
Figure 3.6: A subset of molecularly-defined projection neurons responds to noxious heat stimulation

(A, C, E, G) Representative images of lumbar spinal cord showing retrobead-labeled spinoparabrachial neurons (green) co-expressing *Cck* **(A)***, Nptx2* **(C)***, Nmb* **(E)***,* or *Crh* **(G)** (red), and immediate-early gene *Fos* (blue), after noxious heat stimulation. Insets show enlarged examples of triple-labeled cells. Sections are 12µm thick. Scale bars, 100µm. **(B, D, F, H)** Quantification of experiments in **(A, C, E, G)** represented as pie charts, showing percentages of projection neurons that express *Fos* after noxious heat stimulation (~25-35%), percentage of projection neurons that express *Cck* **(B)***, Nptx2* **(D)***, Nmb* **(F)***,* or *Crh* **(H)**, as well as the percentage of projection neurons that express both *Fos* and the marker gene. Quantification from each marker gene includes data from 2-4 mice, and 3-6 lumbar spinal cord section per mouse.
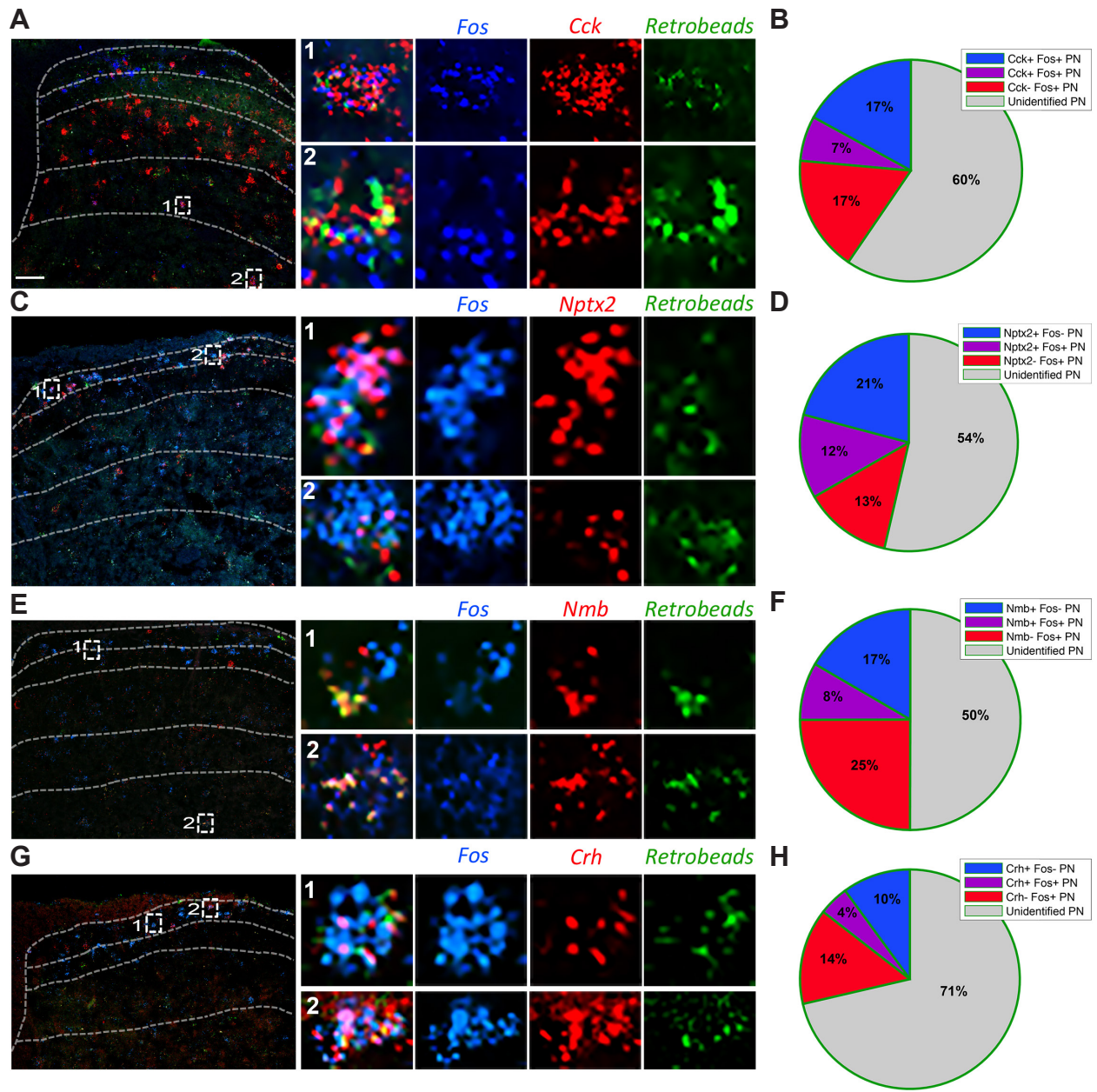
**Figure 3.7: A subset of molecularly-defined projection neurons responds to pruritic stimulation**

(A, C, E, G) Representative images of lumbar spinal cord showing retrobead-labeled spinoparabrachial neurons (green) co-expressing *Cck* **(A)**, *Nptx2* **(C)**, *Nmb* **(E)**, or *Crh* **(G)** (red), and immediate-early gene *Fos* (blue), after pruritic stimulation. Insets show enlarged examples of triple-labeled cells. Sections are 12µm thick. Scale bars, 100µm. **(B, D, F, H)** Quantification of experiments in **(A, C, E, G)** represented as pie charts, showing percentages of projection neurons that express *Fos* after pruritic stimulation (~20-30%), percentage of projection neurons that express *Cck* **(B)**, *Nptx2* **(D)**, *Nmb* **(F)**, or *Crh* **(H)**, as well as the percentage of projection neurons that express both *Fos* and the marker gene. Quantification from each marker gene includes data from 2-4 mice, and 3-6 lumbar spinal cord section per mouse.
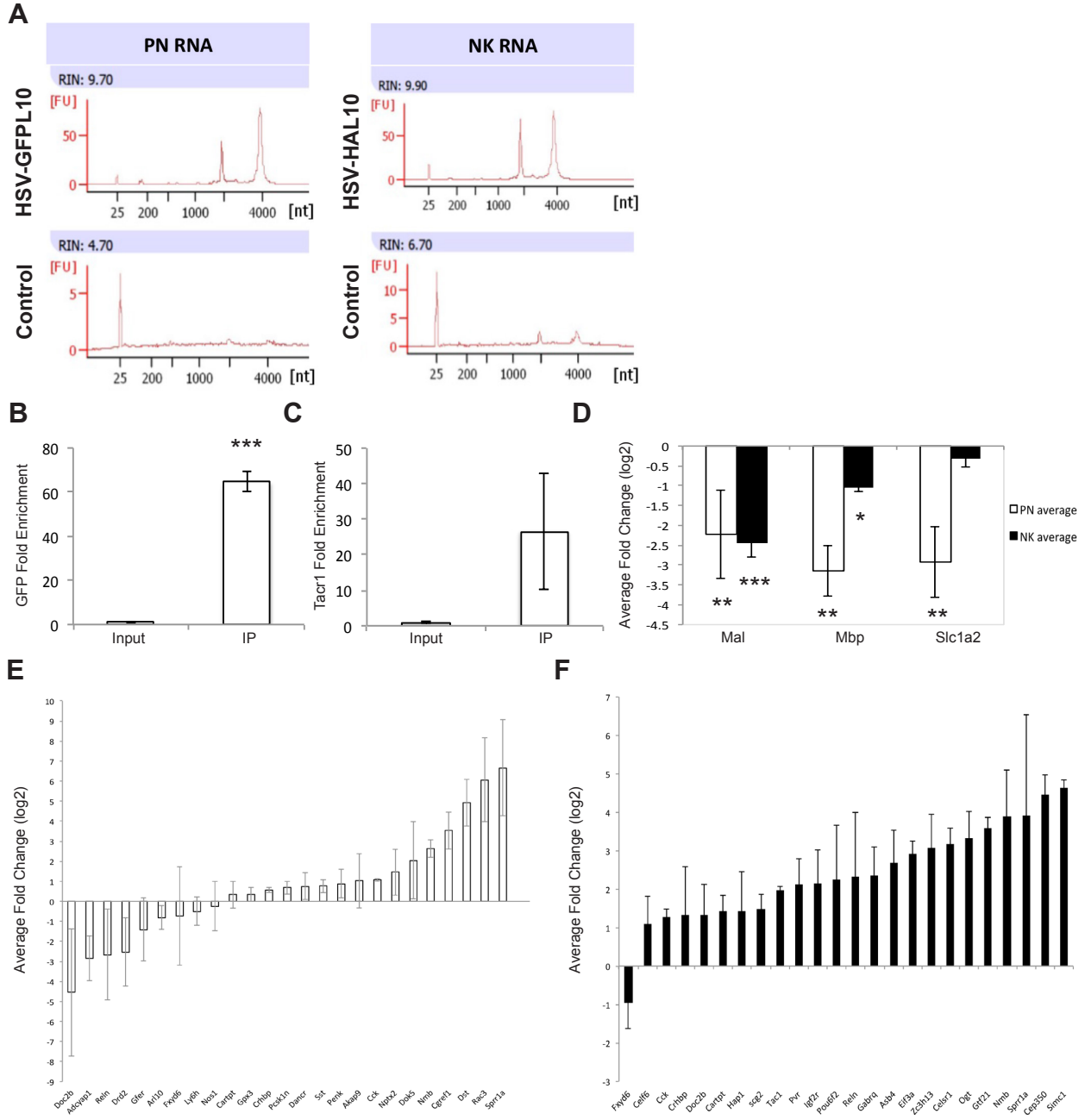
Supplemental Figure 3.1: Validation of RNA purification and sequencing

(A) Bioanalyzer traces of projection neuron IPs from virus injected (top) and control (bottom) animals, for PN (HSV-GFPL10 injected, left) and NK (HSV-HAL10 injected, right) experiments. RIN, RNA Integrity Number. FU, Fluorescence intensity. **(B)** qPCR analysis showing average fold enrichment of *Gfp* mRNA in IP relative to Input from PN experiments. **(C)** qPCR analysis showing average fold enrichment of *Tacr1* mRNA in IP relative to Input from NK experiments. **(D)** qPCR analysis of average glial cell depletion in IPs relative to Input samples for PN and NK experiments. **(E)** qPCR analysis of enriched genes from PN RNAseq dataset **(F)** qPCR analysis of enriched genes from NK dataset **(B-F)** Data are normalized to Rpl27. n = 3 libraries. *$p < 0.05$ **$p < 0.005$ ***$p < 0.0001$
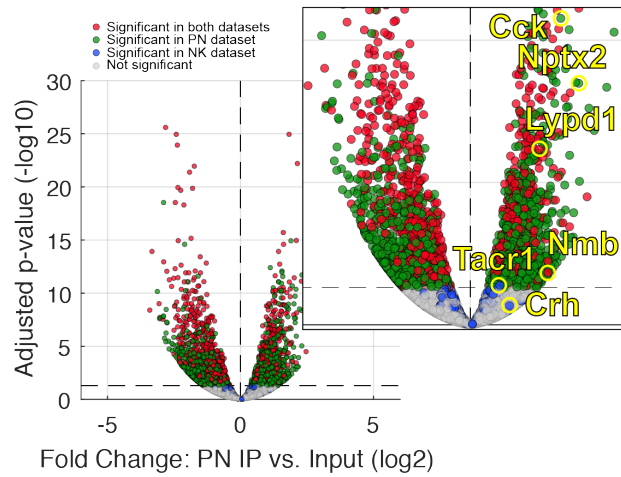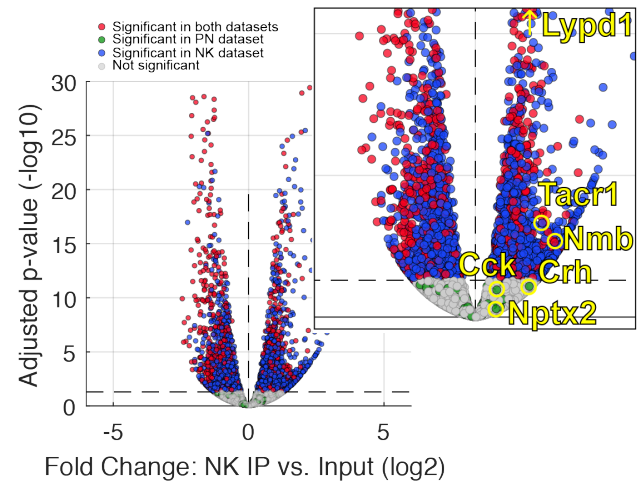
Supplemental Figure 3.2: Volcano plots of RNAseq data: differential expression RNAseq analysis represented as volcano plots for the PN **(A)** and NK experiments **(B)**. Insets show enlarged area with genes of interest highlighted in yellow. Genes significantly changed in both PN and NK datasets are indicated in red, genes significantly changed PN but not NK are shown in green, and genes significantly changed in NK but not PN are shown blue. P < 0.05.
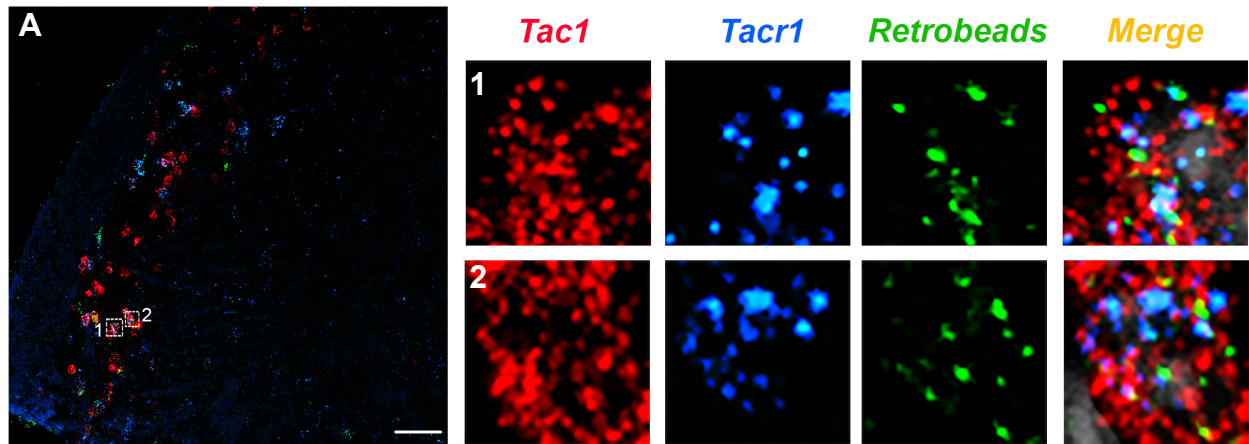
Supplemental Figure 3.3: *Tac1* **is expressed by a subset of NK1R-expressing spinoparabrachial neurons**

(A) Representative section (12µm) showing co-expression of *Tac1* (red) and *Tacr1* (blue) mRNA in retrobead-labeled spinoparabrachial neorons (green). Insets show enlarged examples of triple-labeled cells. Scale bar, 100µm.
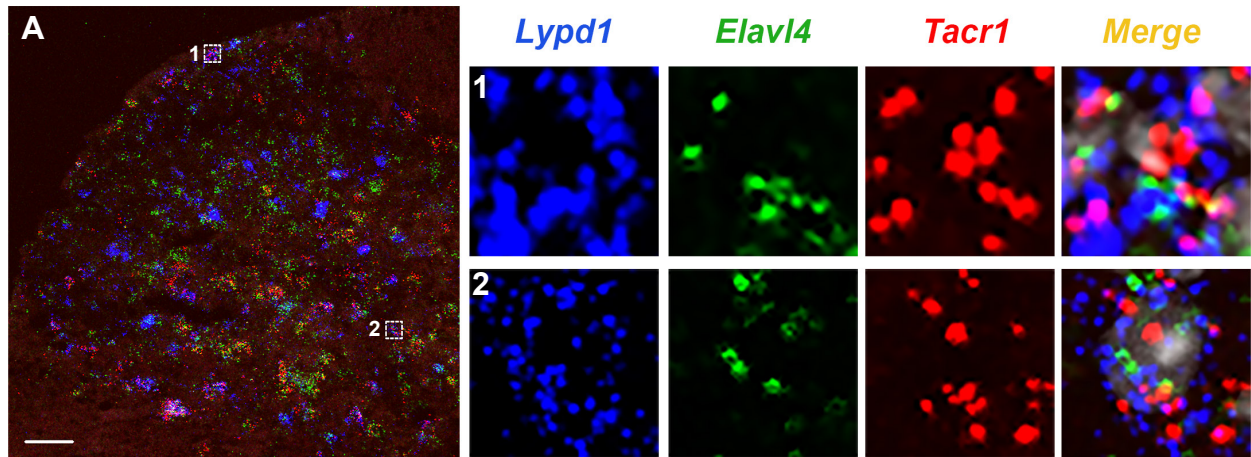
Supplemental Figure 3.4: *Lypd1* and *Elavl4* are expressed by a subset of NK1R-expressing neurons

(A) Representative section (12μm) showing co-expression of *Lypd1* (blue) and *Elavl4* (green) and *Tacr1* (red) mRNA. Insets show enlarged examples of triple-labeled cells. Scale bar, 100μm.
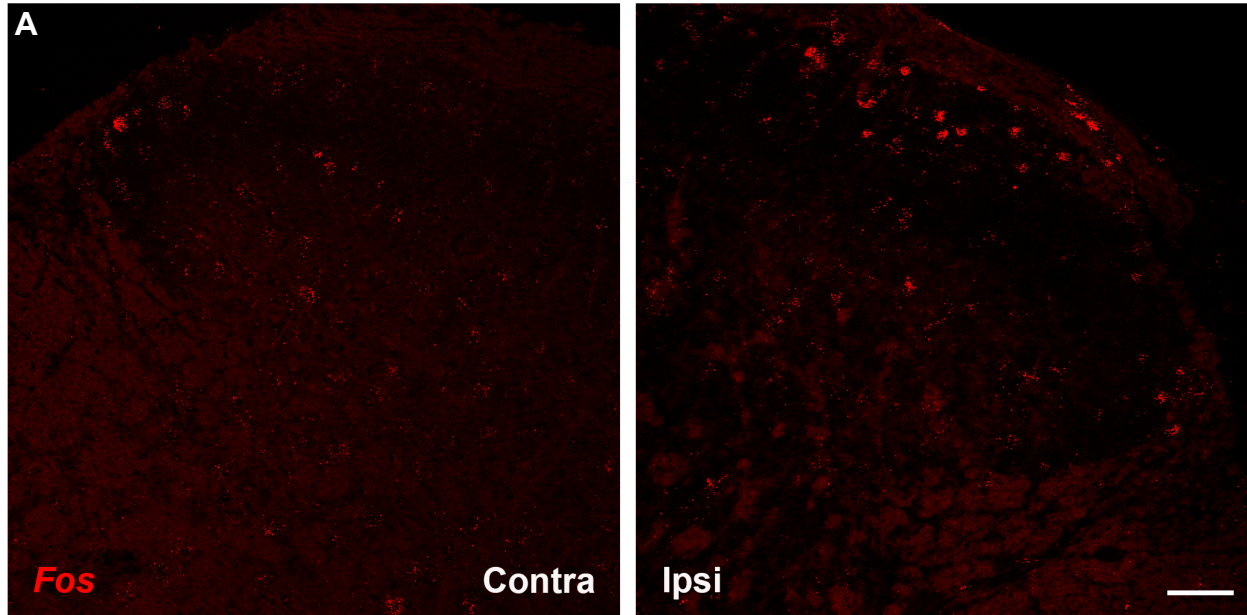
Supplemental Figure 3.5: Noxious Heat stimulation evokes _Fos_ mRNA in ipsilateral superficial dorsal horn

(A) Representative sections of lumbar spinal cord (12µm) showing asymmetrical ipsilateral _Fos_ expression in superficial dorsal horn after noxious heat stimulation. Scale bar, 100µm.
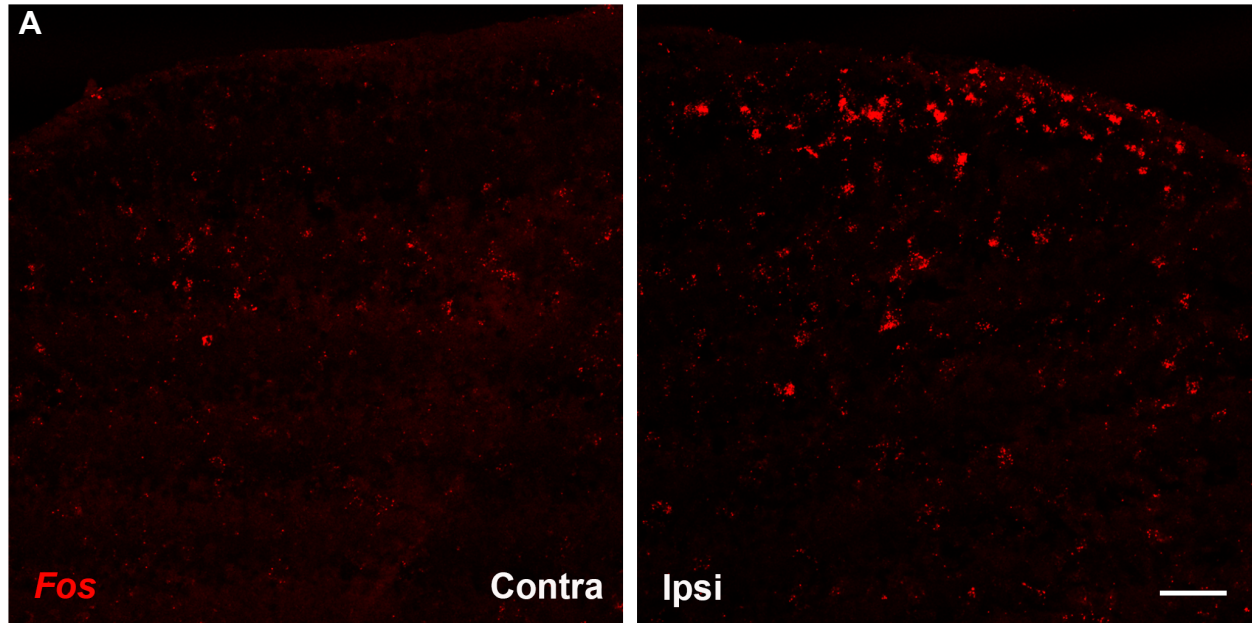
Supplemental Figure 3.6: Pruritic stimulation evokes *Fos* mRNA in ipsilateral TNC
(A) Representative sections of TNC (12µm) showing asymmetrical ipsilateral *Fos*
expression after pruritic stimulation. Scale bar, 100µm.

References

Al-Khater KM, Todd AJ (2009) Collateral projections of neurons in laminae I, III, and IV of rat spinal cord to thalamus, periaqueductal gray matter, and lateral parabrachial area. J Comp Neurol 515:629–646.

Almarestani L, Waters SM, Krause JE, Bennett GJ, Ribeiro-da-Silva A (2007) Morphological characterization of spinal cord dorsal horn lamina I neurons projecting to the parabrachial nucleus in the rat. J Comp Neurol 504:287–297.

Benedetti F, Amanzio M (1997) The neurobiology of placebo analgesia: from endogenous opioids to cholecystokinin. Prog Neurobiol 52:109–125.

Bester H, Chapman V, Besson J-M, Bernard J-F (2000) Physiological Properties of the Lamina I Spinoparabrachial Neurons in the Rat. J Neurophysiol 83:2239–2259.

Blomqvist A, Mackerlova L (1995) Spinal projections to the parabrachial nucleus are substance P-immunoreactive. Neuroreport 6:605–608.

Brown JL, Liu H, Maggio JE, Vigna SR, Mantyh PW, Basbaum AI (1995) Morphological characterization of substance P receptor-immunoreactive neurons in the rat spinal cord and trigeminal nucleus caudalis. J Comp Neurol 356:327–344

Cameron D, Polgár E, Gutierrez-Mecinas M, Gomez-Lima M, Watanabe M, Todd AJ (2015) The organisation of spinoparabrachial neurons in the mouse. Pain 156:2061–2071.

Carstens EE, Carstens MI, Simons CT, Jinks SL (2010) Dorsal horn neurons expressing NK-1 receptors mediate scratching in rats. Neuroreport 21:303–308.

Cavanaugh DJ, Lee H, Lo L, Shields SD, Zylka MJ, Basbaum AI, Anderson DJ (2009) Distinct subsets of unmyelinated primary sensory fibers mediate behavioral responses to noxious thermal and mechanical stimuli. Proc Natl Acad Sci U S A. 106:9075-80.

Chang S, Bok P, Tsai C-Y, Sun C-P, Liu H, Deussing JM, Huang G-J (2018) NPTX2 is a key component in the regulation of anxiety. Neuropsychopharmacology 43:1943–1953.

Christensen B, Perl ER (1970) Spinal neurons specifically excited by noxious or thermal stimuli: marginal zone of the dorsal horn. J Neurophysiol 33:293–307.

Craig AD, Kniffki KD (1985) Spinothalamic lumbosacral lamina I cells responsive to skin and muscle stimulation in the cat. J Physiol 365:197–221.

Craig AD, Krout K, Andrew D (2001) Quantitative response characteristics of thermoreceptive and nociceptive lamina I spinothalamic neurons in the cat. J Neurophysiol 86:1459–1480.

Davidson S, Moser H, Giesler G (2014) Ascending Pathways for Itch. CRC Press/Taylor & Francis. 373.

Davidson S, Zhang X, Khasabov SG, Moser HR, Honda CN, Simone DA, Giesler GJ, Jr. (2012) Pruriceptive spinothalamic tract neurons: physiological properties and projection targets in the primate. J Neurophysiol 108:1711–1723.

Davidson S, Zhang X, Yoon CH, Khasabov SG, Simone DA, Giesler GJ (2007) The itch-producing agents histamine and cowhage activate separate populations of primate spinothalamic tract neurons. J Neurosci 27:10007–10014.

Ding Y-Q, Takada M, Shigemoto R, Mizuno N (1995) Spinoparabrachial tract neurons showing substance P receptor-like immunoreactivity in the lumbar spinal cord of the rat. Brain Res 674:336–340.

Dostrovsky JO, Craig AD (1996) Cooling-specific spinothalamic neurons in the monkey. J Neurophysiol 76:3656–3665.

Duan B, Cheng L, Bourane S, Britz O, Padilla C, Garcia-Campmany L, Krashes M, Knowlton W, Velasquez T, Ren X, Ross SE, Lowell BB, Wang Y, Goulding M, Ma Q (2014) Identification of spinal circuits transmitting and gating mechanical pain. Cell. 159:1417-32.

Ekstrand MI, Nectow AR, Knight ZA, Latcha KN, Pomeranz LE, Friedman JM (2014) Molecular profiling of neurons based on connectivity. Cell. 157:1230-42.

Faris PL, Komisaruk BR, Watkins LR, Mayer DJ (1983) Evidence for the neuropeptide cholecystokinin as an antagonist of opiate analgesia. Science 219:310–312.

Fleming MS, Ramos D, Han SB, Zhao J, Son Y-J, Luo W (2012) The majority of dorsal spinal cord gastrin releasing peptide is synthesized locally whereas neuromedin B is highly expressed in pain- and itch-sensing somatosensory neurons. Mol Pain 8:52.

Gamboa-Esteves FO, McWilliam PN, Batten TF. (2004) Substance P (NK1) and somatostatin (sst2A) receptor immunoreactivity in NTS-projecting rat dorsal horn neurones activated by nociceptive afferent input. J Chem Neuroanat 27:251–266.

Gutierrez-Mecinas M, Bell AM, Shepherd F, Polgár E, Watanabe M, Furuta T, Todd AJ (2019) Expression of cholecystokinin by neurons in mouse spinal dorsal horn. J Comp Neurol:1–15.

Hachisuka J, Baumbauer KM, Omori Y, Snyder LM, Koerber HR, Ross SE (2016) Semi-intact ex vivo approach to investigate spinal somatosensory circuits. Elife 5:1–19.

Han Z-S, Zhang E-T, Craig AD (1998) Nociceptive and thermoreceptive lamina I neurons are anatomically distinct. Nat Neurosci 1:218–225.

Hargreaves KM, Dubner R, Costello AH (1989) Corticotropin releasing factor (CRF) has a peripheral site of action for antinociception. Eur J Pharmacol 170:275–279.

Häring M, Zeisel A, Hochgerner H, Rinwa P, Jakobsson JET, Lönnerberg P, La Manno G, Sharma N, Borgius L, Kiehn O, Lagerström MC, Linnarsson S, Ernfors P (2018) Neuronal atlas of the dorsal horn defines its architecture and links sensory input to transcriptional cell types. Nat Neurosci 21:869–880.

Huang T, Lin S-H, Malewicz NM, Zhang Y, Zhang Y, Goulding M, LaMotte RH, Ma Q (2019) Identifying the pathways required for coping behaviours associated with sustained pain. Nature 565:86–90.

Hylden JLK, Hayashi DRH, Dubner R, Bennett GJ (1986) Physiology and morphology of the lamina I spinomesencephalic projection. J Comp Neurol 247:505–515.

Iggo A, Steedman WM, Fleetwood-Walker S (1985) Spinal processing: anatomy and physiology of spinal nociceptive mechanisms. Philos Trans R Soc London 308:235–252.

Jansen NA, Giesler GJ (2015) Response characteristics of pruriceptive and nociceptive trigeminoparabrachial tract neurons in the rat. J Neurophysiol 113:58–70.

Knowlton WM, Palkar R, Lippoldt EK, McCoy DD, Baluch F, Chen J, McKemy DD
(2013) A Sensory-Labeled Line for Cold: TRPM8-Expressing Sensory Neurons
Define the Cellular Basis for Cold, Cold Pain, and Cooling-Mediated Analgesia. J
Neurosci. 33:2837-48.

Lariviere WR, Melzack R (2000) The role of corticotropin-releasing factor in pain and
analgesia. Pain 84:1–12.

Leah J, Menétrey D, De Pommery J (1988) Neuropeptides in long ascending spinal
tract cells in the rat: Evidence for parallel processing of ascending information.
Neuroscience 24:195–207.

Lima D, Coimbra A (1986) A Golgi study of the neuronal population of the marginal
zone (lamina I) of the rat spinal cord. J Comp Neurol 244:53–71.

Lima D, Coimbra A (1988) The spinothalamic system of the rat: Structural types of
retrogradely labelled neurons in the marginal zone (lamina I). Neuroscience
27:215–230.

Lima D, Coimbra A (1989) Morphological types of spinomesencephalic neurons in the
marginal zone (Lamina I) of the rat spinal cord, as shown after retrograde labelling
with cholera toxin subunit B. J Comp Neurol 279:327–339.

Lima D, Mendes-Ribeiro JA, Coimbra A (1991) The spino-latero-reticular system of the rat: Projections from the superficial dorsal horn and structural characterization of marginal neurons involved. Neuroscience 45:137–152.

Liu Q, Tang Z, Surdenikova L, Kim S, Patel KN, Kim A, Ru F, Guan Y, Weng HJ, Geng Y, Undem BJ, Kollarik M, Chen ZF, Anderson DJ, Dong X (2009) Sensory Neuron-Specific GPCR Mrgprs Are Itch Receptors Mediating Chloroquine-Induced Pruritus. Cell. 139:1353-65.

Ma Q (2012) Population coding of somatic sensations. Neurosci Bull 28:91–99.

Mantyh PW, Rogers SD, Honore P, Allen BJ, Ghilardi JR, Li J, Daughters RS, Lappi DA, Wiley RG, Simone DA (1997) Inhibition of hyperalgesia by ablation of lamina I spinal neurons expressing the substance P receptor. Science 278:275–279.

Marshall GE, Shehab SAS, Spike RC, Todd AJ (1996) Neurokinin-1 receptors on lumbar spinothalamic neurons in the rat. Neuroscience 72:255–263.

McCleane G (2004) Cholecystokinin Antagonists A New Way to Improve the Analgesia from Old Analgesics? Curr Pharm Des 10:303–314.

Mishra SK, Holzman S, Hoon MA (2012) A nociceptive signaling role for neuromedin B. J Neurosci 32:8686–8695.

Miskimon M, Han S, Lee JJ, Ringkamp M, Wilson MA, Petralia RS, Dong X, Worley PF, Baraban JM, Reti IM (2014) Selective expression of Narp in primary nociceptive neurons: Role in microglia/macrophage activation following nerve injury. J Neuroimmunol 274:86–95.

Polgár E, Al-Khater KM, Shehab S, Watanabe M, Todd AJ (2008) Large projection neurons in lamina I of the rat spinal cord that lack the neurokinin 1 receptor are densely innervated by VGLUT2-containing axons and possess GluR4-containing AMPA receptors. J Neurosci 28:13150–13160.

Puskár Z, Polgár E, Todd A. (2001) A population of large lamina I projection neurons with selective inhibitory input in rat spinal cord. Neuroscience 102:167–176.

Sathyamurthy A, Johnson KR, Matson KJE, Dobrott CI, Li L, Ryba AR, Bergman TB, Kelly MC, Kelley MW, Levine AJ (2018) Massively Parallel Single Nucleus Transcriptional Profiling Defines Spinal Cord Neurons and Their Activity during Behavior. Cell Rep. 22:2216-25.

Simone DA, Zhang X, Li J, Zhang J-M, Honda CN, LaMotte RH, Giesler GJ (2004) Comparison of responses of primate spinothalamic tract neurons to pruritic and algogenic stimuli. J Neurophysiol 91:213–222.

Spike RC, Puskár Z, Andrew D, Todd AJ (2003) A quantitative and morphological study of projection neurons in lamina I of the rat lumbar spinal cord. Eur J Neurosci 18:2433–2448.

Su P-Y, Ko M-C (2011) The role of central gastrin-releasing peptide and neuromedin B receptors in the modulation of scratching behavior in rats. J Pharmacol Exp Ther 337:822–829.

Sun YG, Chen ZF (2007) A gastrin-releasing peptide receptor mediates the itch sensation in the spinal cord. Nature. 448:700-703.

Sun YG, Zhao ZQ, Meng XL, Yin J, Liu XY, Chen ZF (2009) Cellular basis of itch sensation. Science. 325:1531-34.

Tekinay AB, Nong Y, Miwa JM, Lieberam I, Ibanez-Tallon I, Greengard P, Heintz N (2009) A role for LYNX2 in anxiety-related behavior. Proc Natl Acad Sci U S A 106:4477–4482.

Todd AJ (2010) Neuronal circuitry for pain processing in the dorsal horn. Nat Rev Neurosci 11:823–836.

Todd AJ, McGill MM, Shehab SAS (2000) Neurokinin 1 receptor expression by neurons in laminae I, III and IV of the rat spinal dorsal horn that project to the brainstem. Eur J Neurosci 12:689–700.

Todd AJ, Spike RC, Polgár E (1998) A quantitative study of neurons which express neurokinin-1 or somatostatin sst(2a) receptor in rat spinal dorsal horn. Neuroscience. 85:459-473.

Wall PD (1967) The laminar organization of dorsal horn and effects of descending impulses. J Physiol 188:403–423.

Wan L, Jin H, Liu X-Y, Jeffry J, Barry DM, Shen K-F, Peng J-H, Liu X-T, Jin J-H, Sun Y, Kim R, Meng Q-T, Mo P, Yin J, Tao A, Bardoni R, Chen Z-F (2017) Distinct roles of NMB and GRP in itch transmission. Sci Rep 7:15466.

Watkins LR, Kinscheck IB, Mayer DJ (1985) Potentiation of morphine analgesia by the cholecystokinin antagonist proglumide. Brain Res 327:169–180.

Willis Jr. WD (1985) Pain pathways in the primate. Prog Clin Biol Res 176:117–133.

Yu XH, Zhang ET, Craig AD, Shigemoto R, Ribeiro-da-Silva A, De Koninck Y (1999) NK-1 receptor immunoreactivity in distinct morphological types of lamina I neurons of the primate spinal cord. J Neurosci 19:3545–3555.

Zhang E-T, Craig AD (1997) Morphology and distribution of spinothalamic lamina I neurons in the monkey. J Neurosci 17:3274–3284.

Zhang E-T, Han Z-S, Craig AD (1996) Morphological classes of spinothalamic lamina I neurons in the cat. J Comp Neurol 367:537–549.

Chapter 4

Conclusions

There is now considerable evidence that segregated somatosensory circuits at the level of the primary afferent and the dorsal horn interneurons, discriminate among pain provoking sensory modalities, e.g. heat, mechanical, chemical, as well as itch. To some extent the functional segregation of these circuits has been associated with specific molecular markers (e.g. TRPV1 for noxious heat responsive sensory neurons, MrgprD for noxious mechanical, and GRP- and GRPR-expressing interneurons that are largely associated with responsiveness to itch-provoking stimuli). On the other hand, our ability to detect specificity and to study comprehensively the functional heterogeneity of the dorsal horn projection neurons is diminished greatly by the relatively low resolution of existing molecular profiles. Here, we addressed this limitation by first molecularly profiling RNA specifically from projection neurons. In these studies we tagged ribosomes of neurons based on established targets for immunoprecipitation (IP) and sequencing. We identified and characterized several enriched genes that define projection neuron subtypes and characterized them according to their coexpression with Tacr1 (the protocypic projection neuron marker), their responsiveness to algogens and pruritogens, and their location in the dorsal horn. Importantly, out study was not restricted to neurons of the superficial dorsal horn, lamina I, where the great majority of previous studies have focused.

Conclusions and Future Directions

Based on the experiments presented here, we conclude that the dorsal horn projection neurons are heterogeneous and are comprised of several subpopulations that can be distinguished based on their expression of different combinations of enriched genes. Although we focused on genes that were particularly enriched in the ribosomal profiles, clearly there are many other genes that need to be examined, for their expression patterns and their functional associations. We determined that there are *Cck+*, *Nptx2+, Nmb+,* and *Crh+* projection neurons that are responsive to pain- and itch-provoking stimuli. This finding shows that there are pain-responsive and itch –responsive projection neurons defined by each enriched gene, but we have not yet established whether "pain" and "itch" messages are transmitted by the same cells, or whether labelled-lines are preserved at the level of the projection neurons. Future experiments are planned to perform highly multiplexed ISH that allow for probing up to 12 genes in a single section, which will permit more extensive combined neuroanatomical and functional analysis. Furthermore, to determine if the molecular subpopulations of projection neurons represent the origin of functionally distinct labeled-lines, we are planning targeted ablation or activation studies (e.g. by using DREADDs or optogenetics). Toward this end, our laboratory is in the process of generating and expanding Nptx2-cre and Tacr1-cre mouse lines, which will permit intersectional approaches (e.g. in combination with LPb injections of retrogradely-transported viruses that express diphtheria toxin receptors or various light activated opsins) to manipulate more precisely the function of subsets of projection neurons.

Publishing Agreement

It is the policy of the University to encourage the distribution of all theses, dissertations, and manuscripts. Copies of all UCSF theses, dissertations, and manuscripts will be routed to the library via the Graduate Division. The library will make all theses, dissertations, and manuscripts accessible to the public and will preserve these to the best of their abilities, in perpetuity.

Please sign the following statement:

I hereby grant permission to the Graduate Division of the University of California, San Francisco to release copies of my thesis, dissertation, or manuscript to the Campus Library to provide access and preservation, in whole or in part, in perpetuity.

_____Racheli Wercberger_____   _____6/12/19_____
Author Signature   Date